

Electronic Supplementary Information

β -Methoxyphenyl Substituted Porphyrins: Synthesis, Characterization and Comprehensive Spectral, Structural, Electrochemical and Theoretical Analysis

Waseem Arif^a, Vipin Kumar^b, Prabhakar Chetti^b and Ravi Kumar*^a

^aDepartment of Chemistry, National Institute of Technology Srinagar, 190006, Jammu and Kashmir, India

^bDepartment of Chemistry, National Institute of Technology Kurukshetra, 136119, Kurukshetra, Haryana, India

Table of Contents (TOC)

Figure S1. UV- Visible spectra of CuTPP(R)₂ ; where R = *p*-CH₃O-Ph, *m*-CH₃O-Ph & *m,p*-CH₃O-Ph in CH₂Cl₂.

Figure S2. UV- Visible spectra of CoTPP(R)₂ ; where R = *p*-CH₃O-Ph, *m*-CH₃O-Ph & *m,p*-CH₃O-Ph in CH₂Cl₂.

Figure S3. UV- Visible spectra of NiTPP(R)₂ ; where R = *p*-CH₃O-Ph, *m*-CH₃O-Ph & *m,p*-CH₃O-Ph in CH₂Cl₂.

Figure S4. UV- Visible spectra of ZnTPP(R)₂ ; where R = *p*-CH₃O-Ph, *m*-CH₃O-Ph & *m,p*-CH₃O-Ph in CH₂Cl₂.

Figure S5. Fluorescence spectra of ZnTPP(R)₂ ; where R = *p*-CH₃O-Ph, *m*-CH₃O-Ph & *m,p*-CH₃O-Ph in CH₂Cl₂ at 298 K.

Figure S6. Cyclic voltammograms of NiTPP(R)₂ ; where R = *p*-CH₃O-Ph, *m*-CH₃O-Ph & *m,p*-CH₃O-Ph (~1 mM) in CH₂Cl₂ containing 0.1 M TBAPF₆ using Ag/AgCl as reference electrode with a scan rate of 0.10 V/s at 298 K.

Figure S7. Cyclic voltammograms of CuTPP(R)₂ ; where R = *p*-CH₃O-Ph, *m*-CH₃O-Ph & *m,p*-CH₃O-Ph (~1 mM) in CH₂Cl₂ containing 0.1 M TBAPF₆ using Ag/AgCl as reference electrode with a scan rate of 0.10 V/s at 298 K.

Figure S8. Cyclic voltammograms of CoTPP(R)₂ ; where R = *p*-CH₃O-Ph, *m*-CH₃O-Ph & *m,p*-CH₃O-Ph (~1 mM) in CH₂Cl₂ containing 0.1 M TBAPF₆ using Ag/AgCl as reference electrode with a scan rate of 0.10 V/s at 298 K.

Figure S9. (a) Represent the dnrm plot, (b) represent the di plot, (c) represent the de plot, (d) represent the shape index (e) represent the curvedness plot and (f) represent the fragment patches with selected network of interaction of ZnTPP(*m*-CH₃O-Ph)₂.

Figure S10. 2D-fingerprint plots showing relative contribution of different types of interactions between atoms in crystal packing of ZnTPP(*m*-CH₃O-Ph)₂. The di and de values are the closest internal and external distances (in Å) from given points on the Hirshfeld surface of ZnTPP(*m*-CH₃O-Ph)₂.

Figure S11. (a) Represent the dnorm plot, (b) represent the di plot, (c) represent the de plot, (d) represent the shape index (e) represent the curvedness plot and (f) represent the fragment patches with selected network of interaction of CuTPP(*m*-CH₃O-Ph)₂.

Figure S12. 2D-fingerprint plots showing relative contribution of different types of interactions between atoms in crystal packing of CuTPP(*m*-CH₃O-Ph)₂. The di and de values are the closest internal and external distances (in Å) from given points on the Hirshfeld surface of CuTPP(*m*-CH₃O-Ph)₂.

Figure S13. Figure S13. Optimized structures of synthesized molecules MTPP(*p*-CH₃O-Ph)₂, M = 2H, Zn (a, b), MTPP(*m*-CH₃O-Ph)₂, M = 2H, Zn (c, d) & MTPP(*m,p*-CH₃O-Ph)₂, M = 2H, Zn (e, f) respectively, by using B3LYP-6-31G (d, p) level of theory in combination with LANL2DZ basis set.

Figure S14. B3LYP/LanL2DZ optimized geometries showing top as well as side views of ZnTPP(*p*-CH₃O-Ph)₂ (a & b), ZnTPP(*m*-CH₃O-Ph)₂ (c & d) and ZnTPP(*m,p*-CH₃O-Ph)₂ (e & f).

Figure S15. B3LYP/6-31G optimized geometries showing direction of dipole moment of MTPP(*p*-CH₃O-Ph)₂, M = 2H, Zn (a, b), MTPP(*m*-CH₃O-Ph)₂, M = 2H, Zn (c, d) & MTPP(*m,p*-CH₃O-Ph)₂, M = 2H, Zn (e, f) respectively. by using B3LYP-6-31G (d, p) level of theory in combination with LANL2DZ basis set Color codes for atoms: C (black), N (blue), H (white) and O (red) and Zn (light blue).

Figure S16. B3LYP/6-31G optimised geometries showing Frontier Molecular Orbitals (FMOs) of H₂TPP(*p*-CH₃O-Ph)₂ (having isosurface contour value of 0.03).

Figure S17. B3LYP/6-31G optimised geometries showing Frontier Molecular Orbitals (FMOs) of ZnTPP(*p*-CH₃O-Ph)₂ (having isosurface contour value of 0.03).

Figure S18. B3LYP/6-31G optimised geometries showing Frontier Molecular Orbitals (FMOs) of H₂TPP(*m*-CH₃O-Ph)₂ (having isosurface contour value of 0.03).

Figure S19. B3LYP/6-31G optimised geometries showing Frontier Molecular Orbitals (FMOs) of ZnTPP(*m*-CH₃O-Ph)₂ (having isosurface contour value of 0.03).

Figure S20. B3LYP/6-31G optimised geometries showing Frontier Molecular Orbitals (FMOs) of H₂TPP(*m,p*-CH₃O-Ph)₂ (having isosurface contour value of 0.03).

Figure S21. B3LYP/6-31G optimised geometries showing Frontier Molecular Orbitals (FMOs) of ZnTPP(*m,p*-CH₃O-Ph)₂ (having isosurface contour value of 0.03).

Figure S22. Molecular electrostatic potential (MEP) Zinc porphyrins:(a) ZnTPP(*p*-CH₃O-Ph)₂ (b) ZnTPP(*m*-CH₃O-Ph)₂ and (c) ZnTPP(*m,p*-CH₃O-Ph)₂ using the B3LYP/ 6 31G (d, p) technique in the Gaussian 16W, in gas phase.

Figure S23. ¹H NMR spectrum of H₂TPP(*p*-CH₃O-Ph)₂ in CDCl₃ at 298 K.

Figure S24. ¹H NMR spectrum of ZnTPP(*p*-CH₃O-Ph)₂ in CDCl₃ at 298 K.

Figure S25. ¹H NMR spectrum of NiTPP(*p*-CH₃O-Ph)₂ in CDCl₃ at 298 K.

Figure S26. ¹H NMR spectrum of H₂TPP(*m*-CH₃O-Ph)₂ in CDCl₃ at 298 K.

Figure S27. ¹H NMR spectrum of ZnTPP(*m*-CH₃O-Ph)₂ in CDCl₃ at 298 K.

Figure S28. ¹H NMR spectrum of NiTPP(*m*-CH₃O-Ph)₂ in CDCl₃ at 298 K.

Figure S29. ¹H NMR spectrum of H₂TPP(*m,p*-CH₃O-Ph)₂ in CDCl₃ at 298 K.

Figure S30. ¹H NMR spectrum of ZnTPP(*m,p*-CH₃O-Ph)₂ in CDCl₃ at 298 K.

Figure S31. ¹H NMR spectrum of NiTPP(*m,p*-CH₃O-Ph)₂ in CDCl₃ at 298 K.

Figure S32. ¹³C NMR spectrum of H₂TPP(*p*-CH₃O-Ph)₂ in CDCl₃ at 298 K.

Figure S33. ¹³C NMR spectrum of H₂TPP(*m*-CH₃O-Ph)₂ in CDCl₃ at 298 K.

Figure S34. ¹³C NMR spectrum of H₂TPP(*m,p*-CH₃O-Ph)₂ in CDCl₃ at 298 K.

Figure S35. X-band EPR Spectra of (a) CoTPP(R)₂; where R = *p*-CH₃O-Ph, *m*-CH₃O-Ph & *m,p*-CH₃O-Ph (b) CuTPP(R)₂ ; where R = *p*-CH₃O-Ph, *m*-CH₃O-Ph & *m,p*-CH₃O-Ph in toluene at 100 K.

Figure S36. HRMS spectrum of H₂TPP(*p*-CH₃O-Ph)₂.

Figure S37. HRMS spectrum of ZnTPP(*p*-CH₃O-Ph)₂.

Figure S38. HRMS spectrum of NiTPP(*p*-CH₃O-Ph)₂.

Figure S39. HRMS spectrum of CuTPP(*p*-CH₃O-Ph)₂.

Figure S40. HRMS spectrum of CoTPP(*p*-CH₃O-Ph)₂.

Figure S41. HRMS spectrum of H₂TPP(*m*-CH₃O-Ph)₂.

Figure S42. HRMS spectrum of ZnTPP(*m*-CH₃O-Ph)₂.

Figure S43. HRMS spectrum of NiTPP(*m*-CH₃O-Ph)₂.

Figure S44. HRMS spectrum of CuTPP(*m*-CH₃O-Ph)₂.

Figure S45. HRMS spectrum of CoTPP(*m*-CH₃O-Ph)₂.

Figure S46. HRMS spectrum of H₂TPP(*m,p*-CH₃O-Ph)₂.

Figure S47. HRMS spectrum of ZnTPP(*m,p*-CH₃O-Ph)₂.

Figure S48. HRMS spectrum of NiTPP(*m,p*-CH₃O-Ph)₂.

Figure S49. HRMS spectrum of CoTPP(*m,p*-CH₃O-Ph)₂.

Figure S50. HRMS spectrum of CuTPP(*m,p*-CH₃O-Ph)₂.

Table S1. Optical absorption spectral data of all the newly synthesized β -di-substituted free base porphyrins as well as their metal complexes functionalized with mono-, di- & tri-substituted methoxyphenyl groups. The values in parentheses refer to log ϵ (ϵ in dm³ mol⁻¹ cm⁻¹).

Table S2. Fluorescence spectral data of ZnTPP(R)₂ ; where R = p-CH₃O-Ph, m-CH₃O-Ph & *m,p*-CH₃O-Ph derivatives in CH₂Cl₂ at 298 K, (Φ_f = quantum yield relative to those of ZnTPP in DCM).

Table S3. Electrochemical redox data of newly synthesized free base β -di-substituted porphyrins functionalized with mono-, di- & tri-substituted methoxyphenyl groups and their metal complexes MTPP(R)₂ ; where M = H₂, Cu(II), Ni(II) & Zn(II) and R = *p*-CH₃O-Ph, *m*-CH₃O-Ph & *m,p*-CH₃O-Ph (in CH₂Cl₂ containing 0.1 M TBAPF₆ with a scan rate of 0.1 V/s at 298 K).

Table S4. Crystal structure data of H₂TPP(*p*-CH₃O-Ph)₂, ZnTPP(*m*-CH₃O-Ph)₂ & CuTPP(*m*-CH₃O-Ph)₂.

Table S5. Selected bond lengths (Å) and bond angles (°) of H₂TPP(*p*-CH₃O-Ph)₂, ZnTPP(*m*-CH₃O-Ph)₂ & CuTPP(*m*-CH₃O-Ph)₂.

Table S6. Selected bond lengths (Å) and bond angles (°) for the B3LYP/6-31G optimized geometries of H₂TPP(*p*-CH₃O-Ph)₂, H₂TPP(*m*-CH₃O-Ph)₂ & H₂TPP(*m,p*-CH₃O-Ph)₂.

Table S7. Selected bond lengths (Å) and bond angles (°) for the B3LYP/6-31G optimized geometries of ZnTPP(*p*-CH₃O-Ph)₂, ZnTPP(*m*-CH₃O-Ph)₂ & ZnTPP(*m,p*-CH₃O-Ph)₂.

Table S8. The calculated Absorption, Oscillator strength, Molecular Transitions (M.T.), % weight contribution (% Ci > 10) of synthesized [ZnTPP(R)₂ R = *p*-CH₃O-Ph, *m*-CH₃O-Ph & *m,p*-CH₃O-Ph] at B3LYP-6-31G (d, p) level of theory in combination with LANL2DZ basis set.

Table S1. Optical absorption spectral data of all the newly synthesized β -di-substituted free base porphyrins as well as their metal complexes functionalized with mono-, di- & tri-substituted methoxyphenyl groups. The values in parentheses refer to $\log \epsilon$ (ϵ in $\text{dm}^3 \text{ mol}^{-1} \text{ cm}^{-1}$).

Porphyrins	Soret band, (nm)	Q band(s), (nm)
H ₂ TPP(p-OCH ₃ -Ph) ₂	425 (5.58)	522 (4.34), 554 (4.02), 594 (3.61), 650 (3.47)
CuTPP(p-OCH ₃ -Ph) ₂	418 (5.58)	537 (4.13)
CoTPP(p-OCH ₃ -Ph) ₂	421 (5.63)	545 (4.39)
NiTPP(p-OCH ₃ -Ph) ₂	424 (5.63)	539 (4.48)
ZnTPP(p-OCH ₃ -Ph) ₂	425 (5.62)	553 (4.35), 589 (3.71)
H ₂ TPP(m-OCH ₃ -Ph) ₂	423 (5.57)	521 (4.32), 557 (4.21), 592 (4.00), 653 (3.47)
CuTPP(m-OCH ₃ -Ph) ₂	421 (5.66)	544 (4.25)
CoTPP(m-OCH ₃ -Ph) ₂	417 (5.62)	536 (4.57)
NiTPP(m-OCH ₃ -Ph) ₂	420 (5.63)	535 (4.49)
ZnTPP(m-OCH ₃ -Ph) ₂	423 (5.60)	552 (4.31), 594 (3.70)
H ₂ TPP(m,p-OCH ₃ -Ph) ₂	421 (5.62)	518 (4.39), 553 (4.19), 593 (3.90), 648 (3.64)
CuTPP(m,p-OCH ₃ -Ph) ₂	417 (5.64)	542 (4.38)
CoTPP(m,p-OCH ₃ -Ph) ₂	414 (5.59)	532 (4.53)
NiTPP(m,p-OCH ₃ -Ph) ₂	423 (5.61)	538 (4.46)
ZnTPP(m,p-OCH ₃ -Ph) ₂	422 (5.65)	551 (4.37), 592 (3.67)

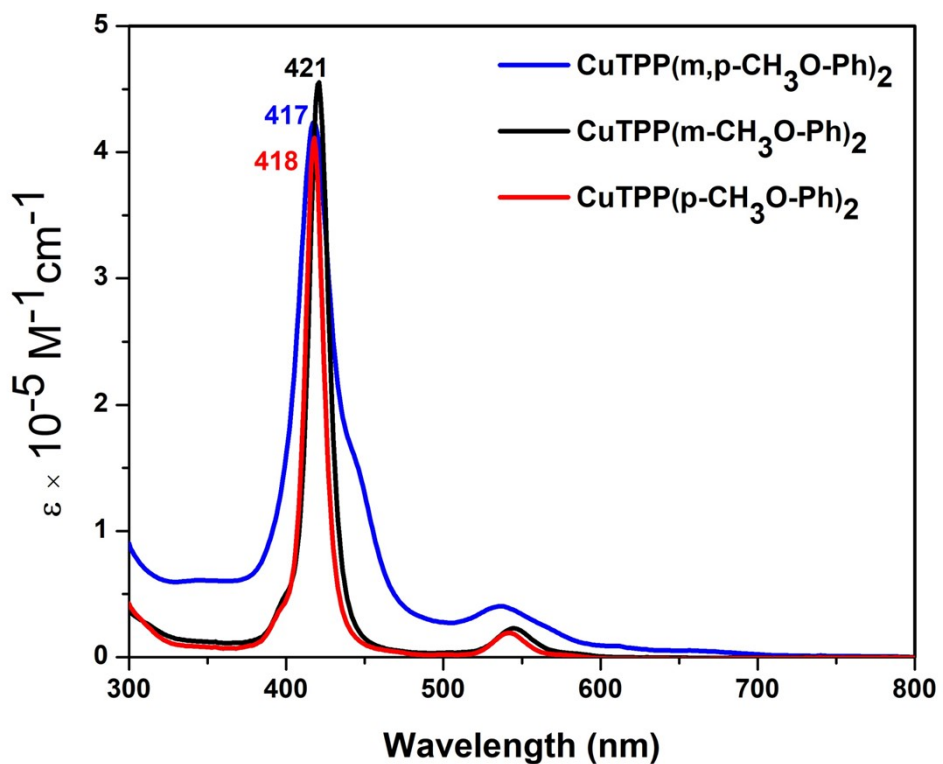


Figure S1. UV- Visible spectra of CuTPP(R)₂ ; where R = *p*-CH₃O-Ph, *m*-CH₃O-Ph & *m,p*-CH₃O-Ph in CH₂Cl₂.

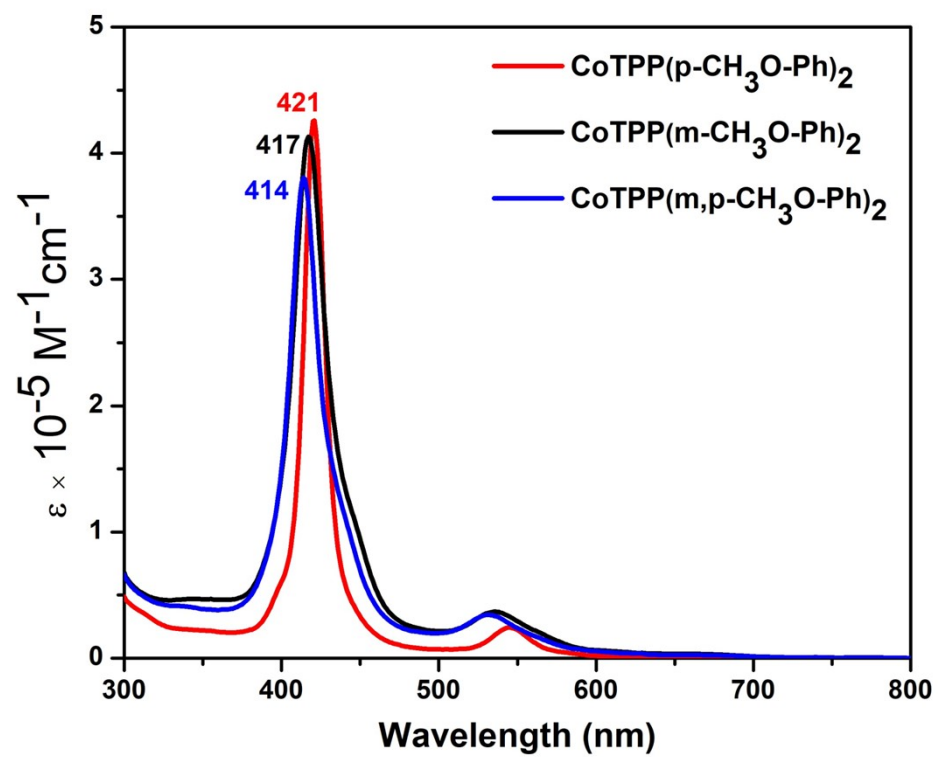


Figure S2. UV- Visible spectra of CoTPP(R)₂ ; where R = *p*-CH₃O-Ph, *m*-CH₃O-Ph & *m,p*-CH₃O-Ph in CH₂Cl₂.

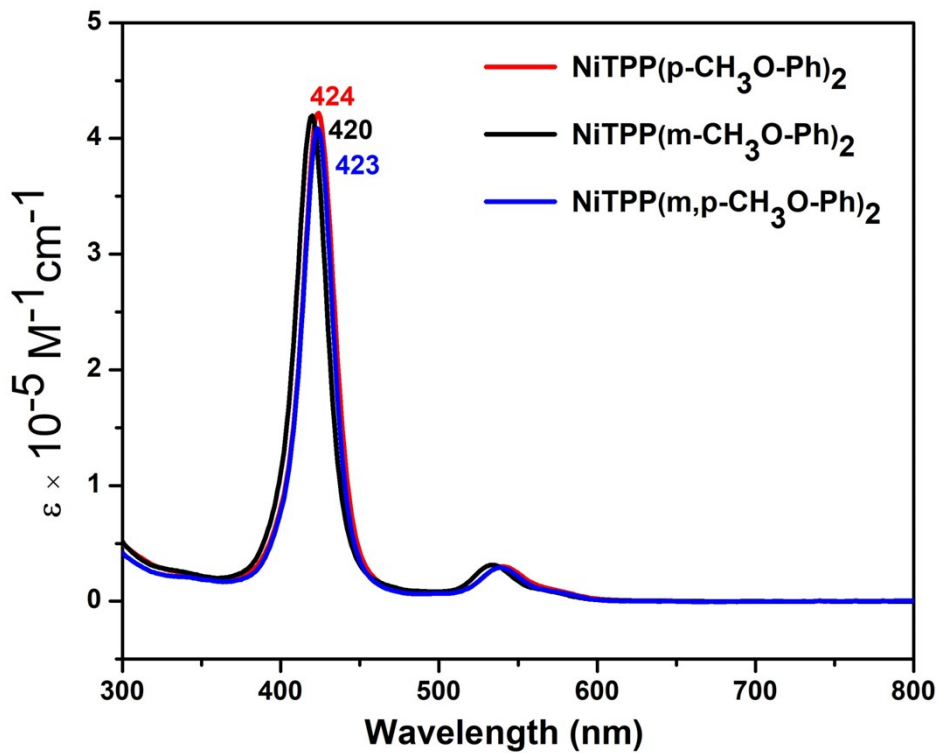


Figure S3. UV- Visible spectra of CoTPP(R)₂ ; where R = *p*-CH₃O-Ph, *m*-CH₃O-Ph & *m,p*-CH₃O-Ph in CH₂Cl₂.

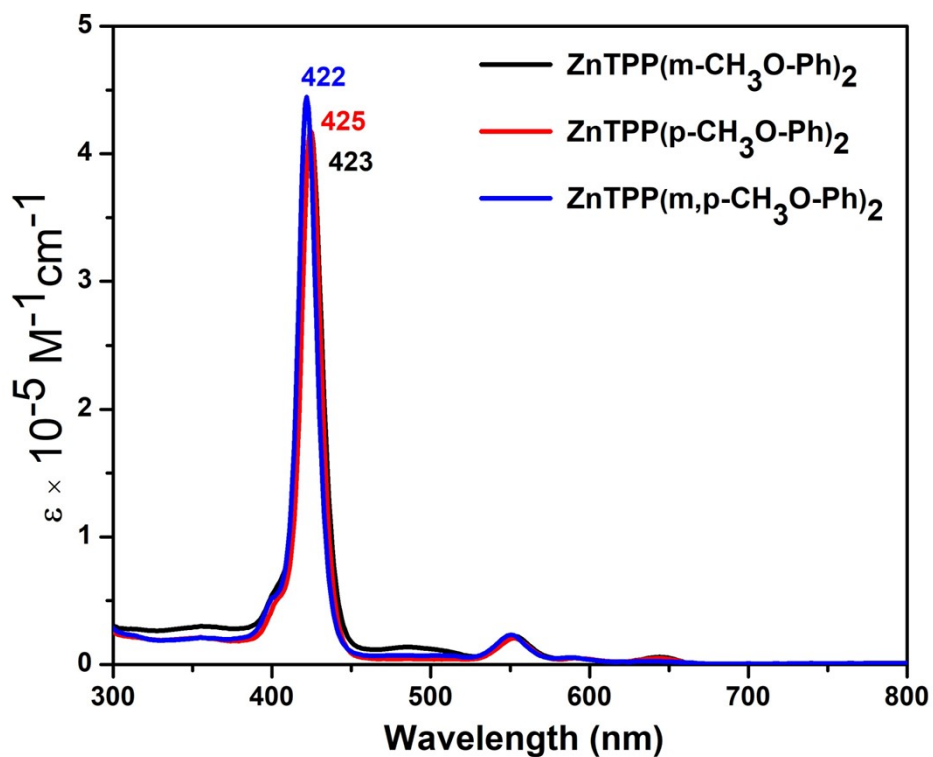


Figure S4. UV- Visible spectra of CoTPP(R)₂ ; where R = *p*-CH₃O-Ph, *m*-CH₃O-Ph & *m,p*-CH₃O-Ph in CH₂Cl₂.

Table S2. Fluorescence spectral data of ZnTPP(R)₂; where R = *p*-CH₃O-Ph, *m*-CH₃O-Ph & *m,p*-CH₃O-Ph derivatives in CH₂Cl₂ at 298 K, (Φ_f = quantum yield relative to those of ZnTPP in DCM).

Porphyrins	λ excitation, nm	λ emission, nm	Φ_f
ZnTPP(<i>p</i> -OCH ₃ -Ph) ₂	424	657	0.0088
ZnTPP(<i>m</i> -OCH ₃ -Ph) ₂	423	656	0.0097
ZnTPP(<i>m,p</i> -OCH ₃ -Ph) ₂	422	654	0.0095

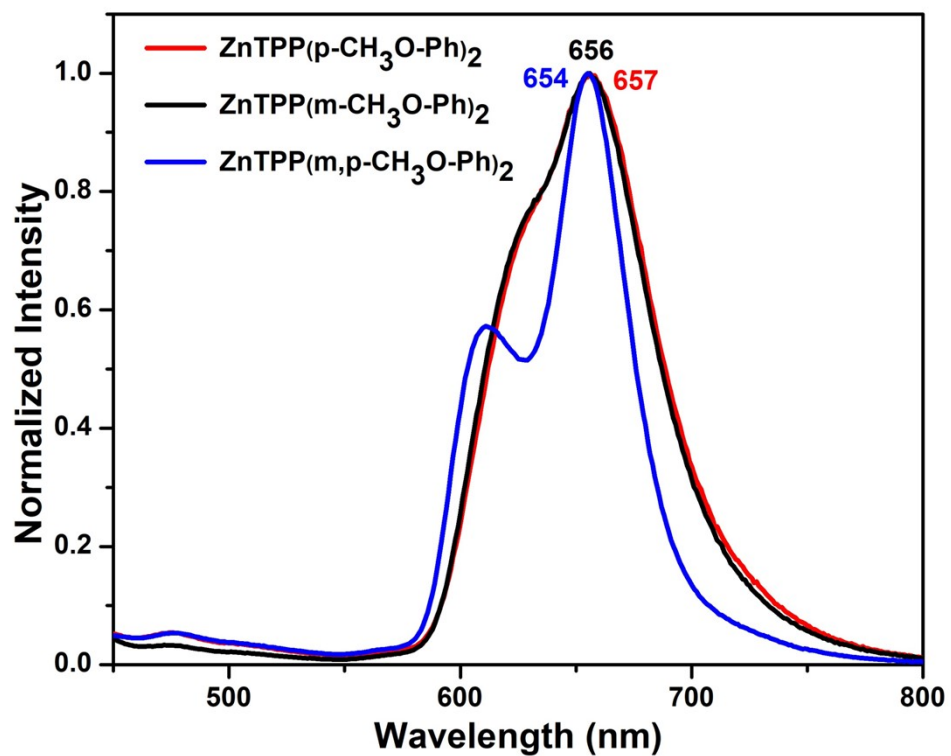


Figure S5. Fluorescence spectra of ZnTPP(R)₂; where R = *p*-CH₃O-Ph, *m*-CH₃O-Ph & *m,p*-CH₃O-Ph in CH₂Cl₂ at 298 K.

Table S3. Electrochemical redox data of newly synthesized free base β -tri-substituted porphyrins functionalized with mono-, di- & tri-substituted methoxyphenyl groups and their metal complexes MTPP(R)₂; where M = H₂, Cu(II), Ni(II) & Zn(II) and R = *p*-CH₃O-Ph, *m*-CH₃O-Ph & *m,p*-CH₃O-Ph (in CH₂Cl₂ containing 0.1 M TBAPF₆ with a scan rate of 0.1 V/s at 298 K).

Porphyrins	Oxidation (V)			Reduction (V)			ΔE (V)
	I-Oxd	II-Oxd	III-Oxd	I-Red	II-Red	III-Red	
H ₂ TPP(p-OCH ₃ -Ph) ₂	0.90	1.08		-1.19	-1.65 ^a		2.08
CuTPP(p-OCH ₃ -Ph) ₂	0.86	1.25		-1.31	-1.67 ^a		2.17
CoTPP(p-OCH ₃ -Ph) ₂	0.65	1.06	1.23	-0.73 ^a	-1.31	-1.39 ^a	2.37
NiTPP(p-OCH ₃ -Ph) ₂	0.95	1.23		-1.27	-1.87 ^a		2.22
ZnTPP(p-OCH ₃ -Ph) ₂	0.76	0.98		-1.37	-1.62 ^a		2.13
H ₂ TPP(m-OCH ₃ -Ph) ₂	0.94	1.09 ^a		-1.19	-1.41		2.13
CuTPP(m-OCH ₃ -Ph) ₂	0.88	1.32	1.51	-1.29	-1.67 ^a		2.17
CoTPP(m-OCH ₃ -Ph) ₂	0.71	1.09	1.37	-0.84	-1.15	-1.38	2.24
NiTPP(m-OCH ₃ -Ph) ₂	1.03	1.29	1.46	-1.11	-1.31	-1.71	2.14
ZnTPP(m-OCH ₃ -Ph) ₂	0.80	1.03		-1.36	-1.58 ^a		2.17
H ₂ TPP(m,p-OCH ₃ -Ph) ₂	1.01	1.24	1.47	-1.22	-1.52 ^a		2.22
CuTPP(m,p-OCH ₃ -Ph) ₂	0.95	1.31	1.46	-1.12	-1.35		2.01
CoTPP(m,p-OCH ₃ -Ph) ₂	0.82	1.08	1.27	-0.84	-1.16	-1.41	2.24
NiTPP(m,p-OCH ₃ -Ph) ₂	0.99	1.27	1.46	-1.32	-1.76	-1.95 ^a	2.31
ZnTPP(m,p-OCH ₃ -Ph) ₂	0.83	1.09	1.45	-1.35	-1.57		2.18

^arefers to the values taken from DPV experiment

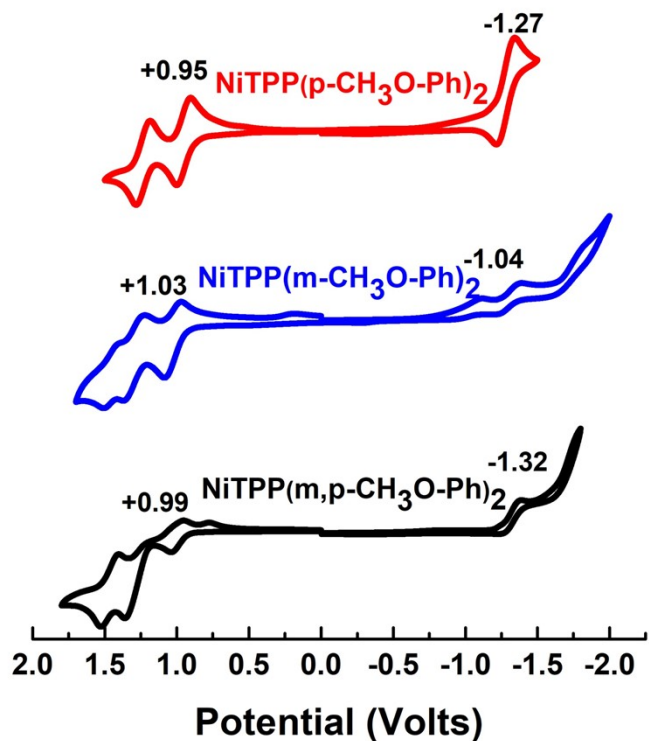


Figure S6. Cyclic voltammograms of $\text{NiTPP}(\text{R})_2$; where $\text{R} = \text{p-CH}_3\text{O-Ph}$, $\text{m-CH}_3\text{O-Ph}$ & $\text{m,p-CH}_3\text{O-Ph}$ (~1 mM) in CH_2Cl_2 containing 0.1 M TBAPF₆ using Ag/AgCl as reference electrode with a scan rate of 0.10 V/s at 298 K.

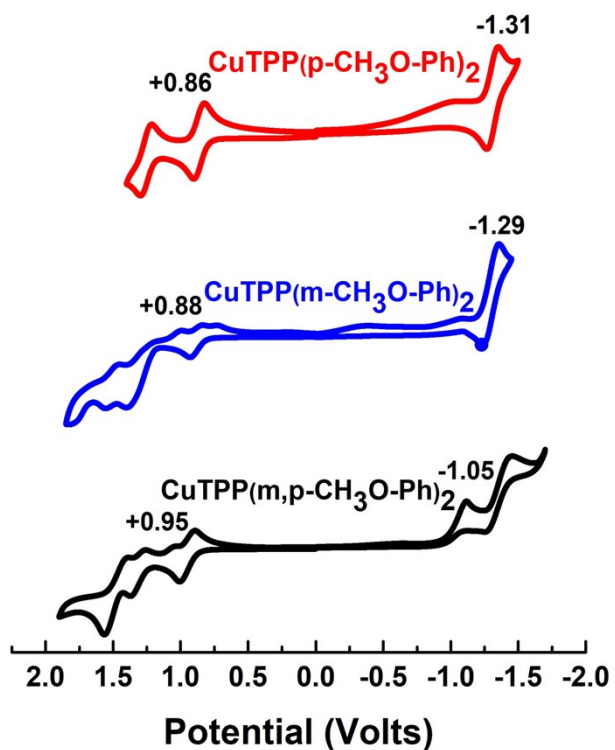


Figure S7. Cyclic voltammograms of $\text{CuTPP}(\text{R})_2$; where $\text{R} = \text{p-CH}_3\text{O-Ph}$, $\text{m-CH}_3\text{O-Ph}$ & $\text{m,p-CH}_3\text{O-Ph}$ (~1 mM) in CH_2Cl_2 containing 0.1 M TBAPF₆ using Ag/AgCl as reference electrode with a scan rate of 0.10 V/s at 298 K.

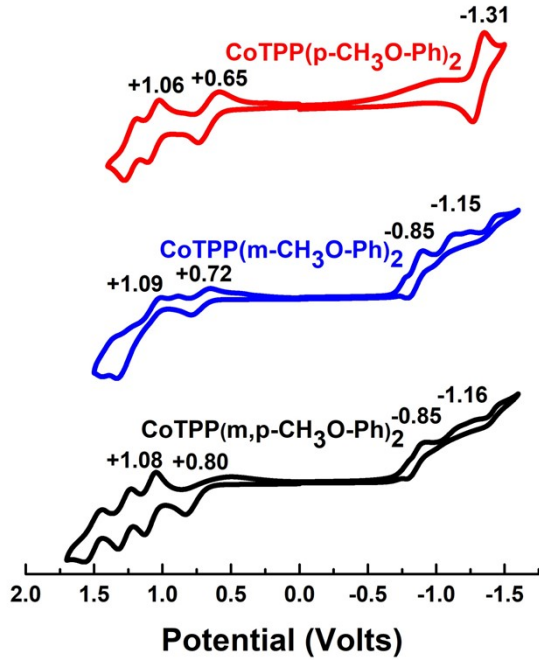
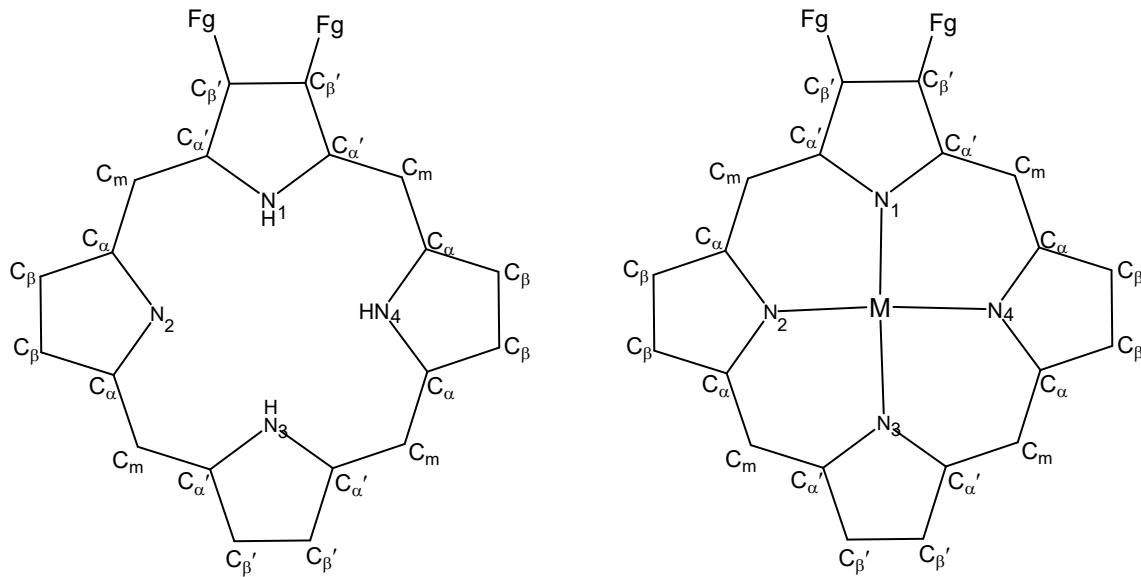


Figure S8. Cyclic voltammograms of $\text{CoTPP}(\text{R})_2$; where $\text{R} = p\text{-CH}_3\text{O-Ph}$, $m\text{-CH}_3\text{O-Ph}$ & $m,p\text{-CH}_3\text{O-Ph}$ (~ 1 mM) in CH_2Cl_2 containing 0.1 M TBAPF_6 using Ag/AgCl as reference electrode with a scan rate of 0.10 V/s at 298 K.

	$\text{H}_2\text{TPP}(p\text{-CH}_3\text{O-Ph})_2$	$\text{ZnTPP}(m\text{-CH}_3\text{O-Ph})_2$	$\text{CuTPP}(m\text{-CH}_3\text{O-Ph})_2$
Empirical formula	$\text{C}_{58}\text{H}_{42}\text{N}_4\text{O}_2$	$\text{C}_{65}\text{H}_{49}\text{N}_5\text{O}_4\text{Zn}$	$\text{C}_{60}\text{H}_{44}\text{N}_4\text{O}_4\text{Cu}$
Formula wt.	826.95	1029.46	948.53
Crystal system	Monoclinic	Monoclinic	Triclinic
Space group	$\text{C}2/\text{c}$	$\text{P}2_1/\text{c}$	$\text{P}-1$
a (Å)	$25.4032(11)$ Å	$9.9765(3)$ Å	$13.2014(7)$ Å
b (Å)	$10.7091(5)$ Å	$41.7796(16)$ Å	$13.3397(7)$ Å
c (Å)	$36.4314(15)$ Å	$13.3216(5)$ Å	$14.8686(7)$ Å
α (°)	90°	90°	$65.629(2)^\circ$
β (°)	$109.790(2)^\circ$	$107.3030(10)$	$76.969(2)^\circ$
γ (°)	90°	90°	$89.430(2)^\circ$
Volume (Å ³)	$9325.6(7)$ Å ³	$5301.3(3)$ Å ³	$2313.5(2)$ Å ³
Z	8	4	2
D_{calc} (Mg/m ³)	1.178 Mg/m ³	1.290 Mg/m ³	1.362 Mg/m ³
Wavelength (Å)	1.54178 Å	0.71073 Å	0.71073 Å
T (K)	$296(2)$ K	$298(2)$ K	$298(2)$ K
No. of total reflns.	62109	101253	99719
No. of indepnt.reflns.	8097	9304	10063
R ^a	0.0721	0.0892	0.0415
R ^b	0.1922	0.1759	0.0946
Theta range for data collection	2.578 to 66.492° .	2.894 to 22.000° .	2.876 to 26.994° .
Crystal size	$0.540 \times 0.051 \times 0.023$ mm ³	$0.550 \times 0.080 \times 0.037$ mm ³	$0.540 \times 0.110 \times 0.032$ mm ³
Refinement method	Full-matrix least-squares on F^2	Full-matrix least-squares on F^2	Full-matrix least-squares on F^2
CCDC	2281590	2331012	2331015

Table S4. Crystal structure data of H₂TPP(*p*-CH₃O-Ph)₂, ZnTPP(*m*-CH₃O-Ph)₂ & CuTPP(*m*-CH₃O-Ph)₂.

Table S5. Selected bond lengths (Å) and bond angles (°) of H₂TPP(*p*-CH₃O-Ph)₂, ZnTPP(*m*-CH₃O-Ph)₂ & CuTPP(*m*-CH₃O-Ph)₂.



Bond Length (Å)

	H ₂ TPP(<i>p</i> -CH ₃ O-Ph) ₂	ZnTPP(<i>m</i> -CH ₃ O-Ph) ₂	CuTPP(<i>m</i> -CH ₃ O-Ph) ₂
M-N	-	2.065 (6)	1.987 (2)
M-N'	-	2.102 (6)	1.999 (2)
N-C _α	1.381 (4)	1.377 (7)	1.380 (4)
N'-C _{α'}	1.371 (3)	1.375 (7)	1.379 (3)
C _α -C _β	1.445 (4)	1.446 (8)	1.435 (3)
C _α -C _{β'}	1.444 (4)	1.452 (7)	1.444 (2)
C _β -C _β	1.344 (5)	1.343 (5)	1.348 (3)
C _β -C _{β'}	1.357 (4)	1.351 (8)	1.351 (3)
C _α -C _m	1.397 (5)	1.406 (6)	1.397 (3)
C _α -C _m	1.401 (4)	1.409 (5)	1.395 (2)
ΔC _β (Å) ^a	0.014	0.128	0.558
Δ24(Å) ^b	0.021	0.098	0.286
ΔMetal(Å)	-	0.379	0.066

Bond Angle (deg)

M-N-C _α	-	125.77 (5)	126.29 (3)
M-N'-C _α	-	126.07 (6)	126.59 (4)
N-M-N	-	161.63 (10)	173.82 (7)
N'-M-N'	-	160.78 (12)	177.57 (9)
N-C _α -C _m	126.77 (4)	126.24 (6)	125.39 (2)
N'-C _{α'} -C _m	126.30 (5)	125.37 (7)	124.63 (3)

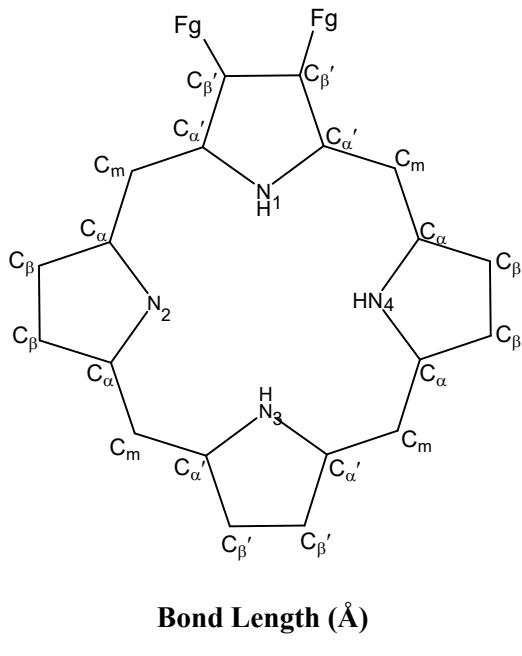
N-C _α -C _β	109.65 (3)	109.32 (4)	109.78 (2)
N'-C _{α'} -C _{β'}	106.62 (4)	108.92 (5)	109.67 (4)
C _β -C _α -C _m	123.45 (4)	124.37 (5)	124.66 (3)
C _{β'} -C _{α'} -C _m	127.31 (5)	125.66 (4)	125.49 (3)
C _α -C _m -C _{α'}	125.42 (6)	125.15 (6)	123.31 (2)
C _α -C _β -C _β	107.35 (4)	107.39 (7)	107.24 (2)
C _{α'} -C _{β'} -C _{β'}	108.11 (4)	107.47 (4)	107.17 (3)
C _α -N-C _α	105.99 (5)	106.54 (6)	105.70 (4)
C _α -N-C _{α'}	110.52 (5)	107.41 (6)	106.02 (4)

^aΔC_β refers to the mean plane displacement of the β-pyrrole carbons

^bΔ24 refers to the mean plane deviation of 24-atom core

esd's for all given bond length and bond angles are ± 5%

Table S6. Selected bond lengths (Å), bond angles (°) and dipole moments for the B3LYP/6-31G optimized geometries of H₂TPP(*p*-CH₃O-Ph)₂, H₂TPP(*m*-CH₃O-Ph)₂ & H₂TPP(*m,p*-CH₃O-Ph)₂.



Bond Length (Å)

	H ₂ TPP(<i>p</i> -CH ₃ O-Ph) ₂	H ₂ TPP(<i>m</i> -CH ₃ O-Ph) ₂	H ₂ TPP(<i>m,p</i> -CH ₃ O-Ph) ₂
N-C _α	1.366	1.365	1.367
N'-C _{α'}	1.375	1.372	1.375
C _α -C _β	1.460	1.413	1.459
C _{α'} -C _{β'}	1.439	1.408	1.439
C _β -C _β	1.353	1.352	1.351
C _{β'} -C _{β'}	1.380	1.379	1.380
C _α -C _m	1.413	1.460	1.416
C _{α'} -C _m	1.409	1.439	1.412
ΔC _β (Å) ^a	0.430	0.480	0.490
Δ24(Å) ^b	0.220	0.232	0.241

Bond Angle (deg)

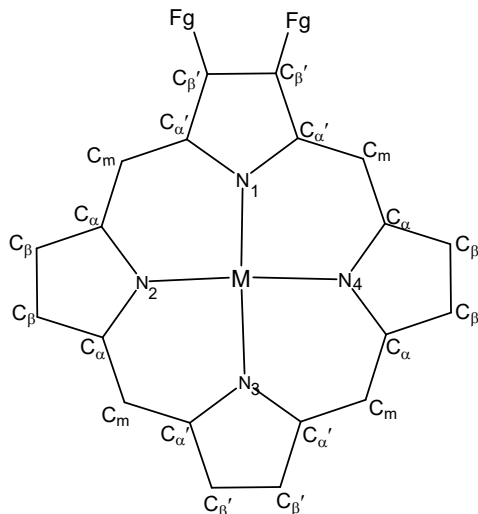
	H ₂ TPP(<i>p</i> -CH ₃ O-Ph) ₂	H ₂ TPP(<i>m</i> -CH ₃ O-Ph) ₂	H ₂ TPP(<i>m,p</i> -CH ₃ O-Ph) ₂
N-C _α -C _m	126.15	126.23	126.29
N'-C _{α'} -C _m	125.31	125.41	125.25
N-C _α -C _β	110.85	110.86	110.61
N'-C _{α'} -C _{β'}	106.46	106.43	106.40
C _β -C _α -C _m	122.95	122.87	122.80
C _{β'} -C _{α'} -C _m	128.17	127.62	128.27
C _α -C _m -C _{α'}	124.80	124.82	124.85
C _α -C _β -C _β	106.35	106.35	106.35
C _{α'} -C _{β'} -C _{β'}	107.93	107.95	107.96
C _α -C _n -C _α	105.51	105.49	105.85
C _{α'} -C _n -C _{α'}	111.05	111.09	111.12
Dipole moment	2.3734 D	5.1528 D	2.7013 D

^aΔC_β refers to the mean plane displacement of the β-pyrrole carbons

^bΔ24 refers to the mean plane deviation of 24-atom core

esd's for all given bond length and bond angles are ± 5%

Table S7. Selected bond lengths (Å), bond angles (°) and dipole moment for the B3LYP/LANL2DZ optimized geometries of ZnTPP(*p*-CH₃O-Ph)₂, ZnTPP(*m*-CH₃O-Ph)₂ & ZnTPP(*m,p*-CH₃O-Ph)₂.



Bond Length (Å)

	ZnTPP(<i>p</i> -CH ₃ O-Ph) ₂	ZnTPP(<i>m</i> -CH ₃ O-Ph) ₂	ZnTPP(<i>m,p</i> -CH ₃ O-Ph) ₂
M-N	2.058	2.055	2.053
M-N'	2.083	2.087	2.081
N-C _α	1.375	1.376	1.378
N'-C _{α'}	1.375	1.374	1.372
C _α -C _β	1.446	1.447	1.449
C _{α'} -C _{β'}	1.452	1.453	1.456
C _β -C _β	1.364	1.362	1.360
C _{β'} -C _{β'}	1.371	1.369	1.365
C _α -C _m	1.412	1.412	1.412
C _{α'} -C _m	1.414	1.416	1.416
ΔC _β (Å) ^a	0.425	0.388	0.370
Δ24(Å) ^b	0.203	0.186	0.177
ΔMetal(Å)	0.017	0.014	0.016

Bond Angle (deg)

	ZnTPP(<i>p</i> -CH ₃ O-Ph) ₂	ZnTPP(<i>m</i> -CH ₃ O-Ph) ₂	ZnTPP(<i>m,p</i> -CH ₃ O-Ph) ₂
M-N-C _α	125.62	125.76	125.821
M-N'-C _α	125.63	125.68	125.73
N-M-N	179.04	179.27	179.23
N'-M-N'	179.25	179.40	179.47
N-C _α -C _m	126.05	126.17	126.21
N'-C _{α'} -C _m	124.93	124.91	124.95
N-C _α -C _β	109.06	109.07	109.53
N'-C _{α'} -C _{β'}	109.25	109.19	109.19
C _β -C _α -C _m	124.86	124.73	124.69
C _{β'} -C _{α'} -C _m	125.80	125.86	125.83
C _α -C _m -C _{α'}	125.37	125.22	125.52
C _α -C _β -C _β	107.20	107.24	107.28
C _{α'} -C _{β'} -C _{β'}	106.92	106.94	106.87
C _α -C _n -C _α	107.41	107.43	107.42
C _{α'} -C _n -C _{α'}	107.52	107.57	107.58
Dipole moment	2.313 D	2.203 D	2.871 D

^aΔC_β refers to the mean plane displacement of the β-pyrrole carbons

^bΔ24 refers to the mean plane deviation of 24-atom core

esd's for all given bond length and bond angles are $\pm 5\%$

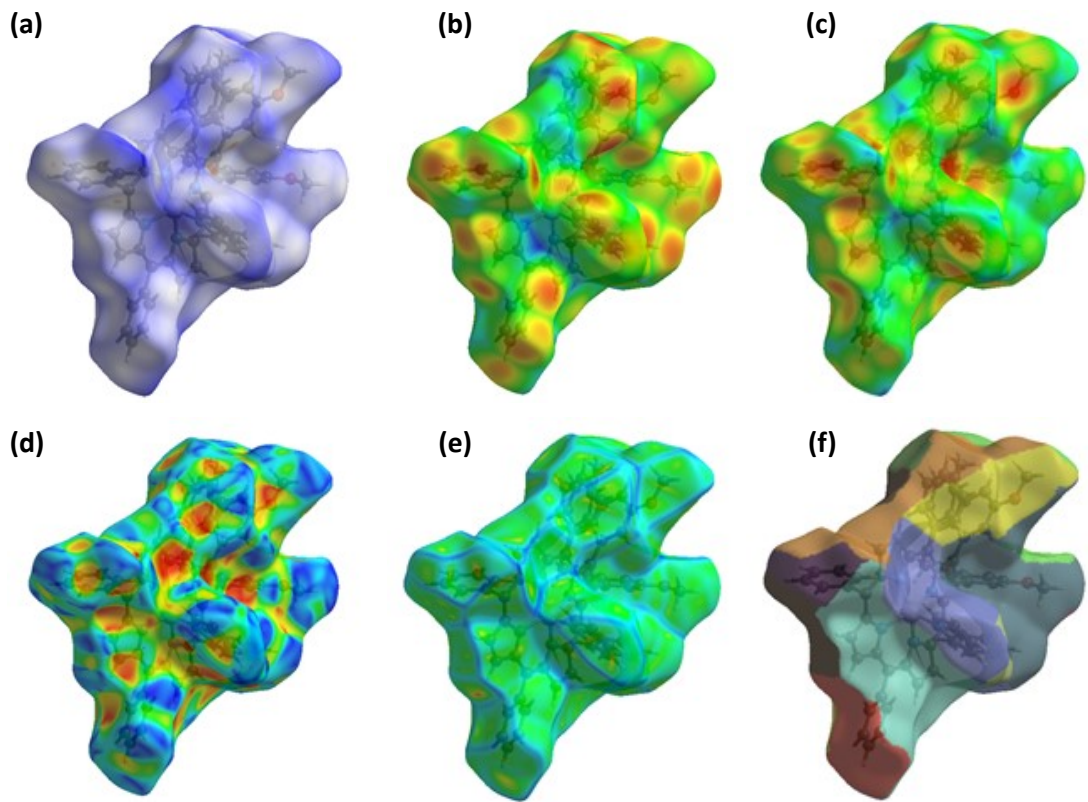


Figure S9. (a) Represent the dnorm plot, (b) represent the di plot, (c) represent the de plot, (d) represent the shape index (e) represent the curvedness plot and (f) represent the fragment patches with selected network of interaction of ZnTPP(*m*-CH₃O-Ph)₂.

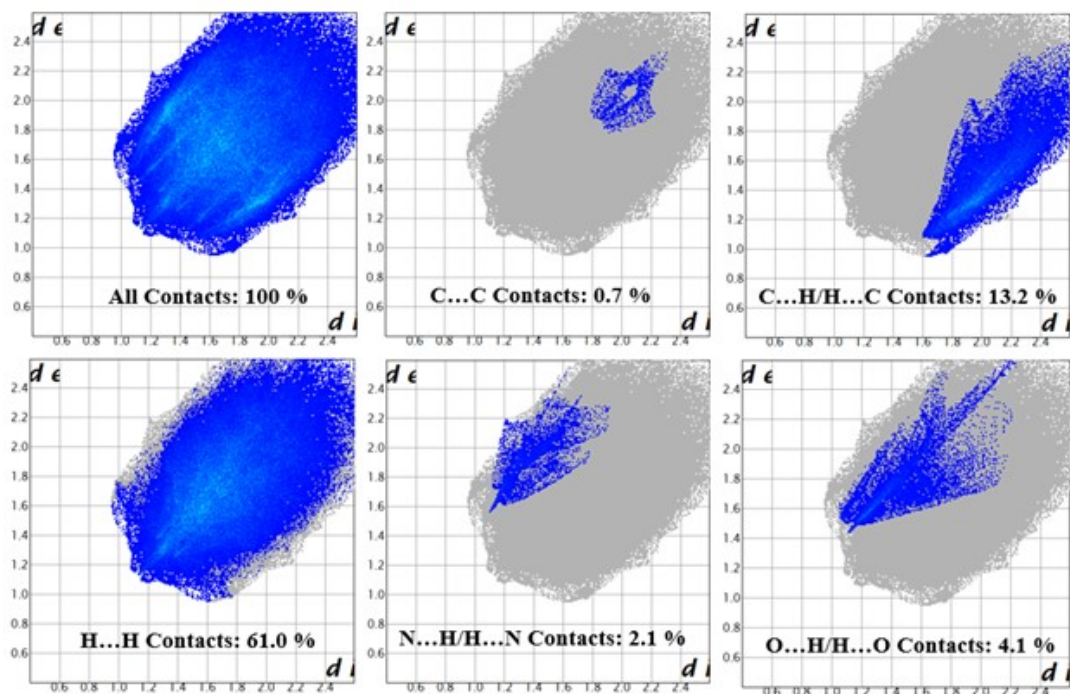


Figure S10. 2D-fingerprint plots showing relative contribution of different types of interactions between atoms in crystal packing of ZnTPP(*m*-CH₃O-Ph)₂. The di and de values are the closest

internal and external distances (in Å) from given points on the Hirshfeld surface of ZnTPP(*m*-CH₃O-Ph)₂.

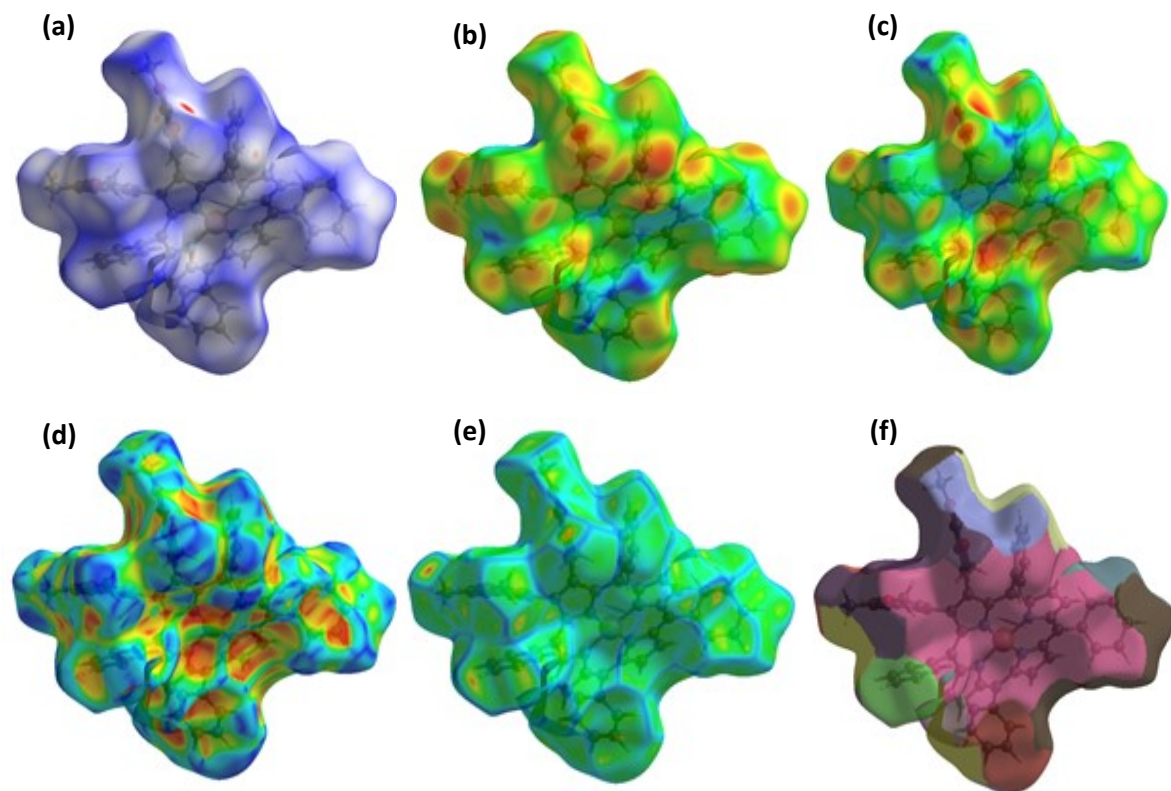


Figure S11. (a) Represent the dnorm plot, (b) represent the di plot, (c) represent the de plot, (d) represent the shape index (e) represent the curvedness plot and (f) represent the fragment patches with selected network of interaction of CuTPP(*m*-CH₃O-Ph)₂.

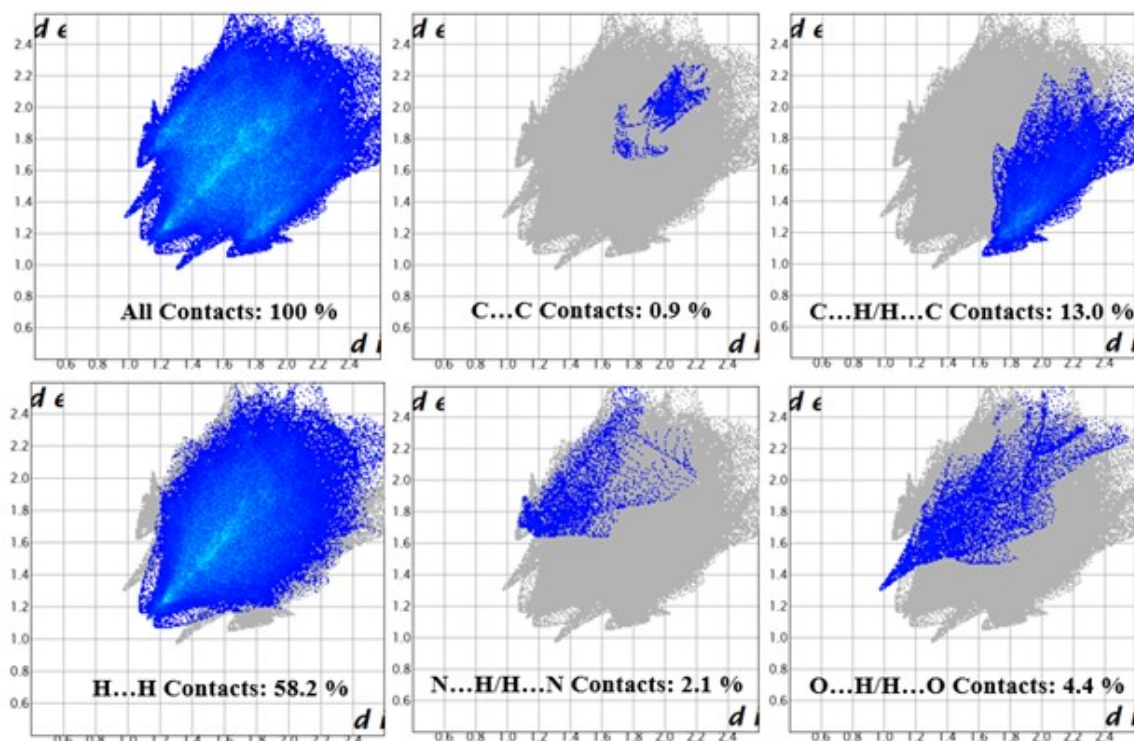


Figure S12. 2D-fingerprint plots showing relative contribution of different types of interactions between atoms in crystal packing of CuTPP(*m*-CH₃O-Ph)₂. The di and de values are the closest internal and external distances (in Å) from given points on the hirshfeld surface of CuTPP(*m*-CH₃O-Ph)₂.

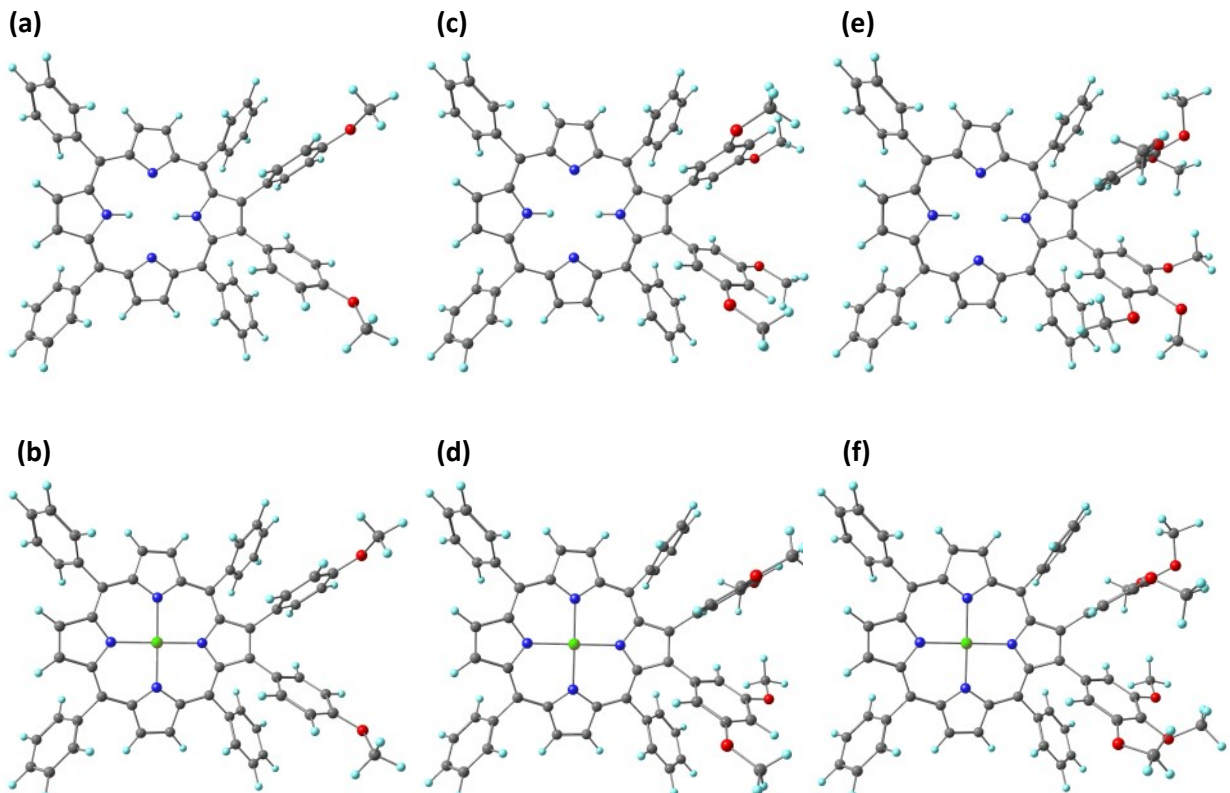


Figure S13. Optimized structures of synthesized molecules MTPP(*p*-CH₃O-Ph)₂, M = 2H, Zn (a, b), MTPP(*m*-CH₃O-Ph)₂, M = 2H, Zn (c, d) & MTPP(*m,p*-CH₃O-Ph)₂, M = 2H, Zn (e, f) respectively, by using B3LYP-6-31G (d, p) level of theory in combination with LANL2DZ basis set.

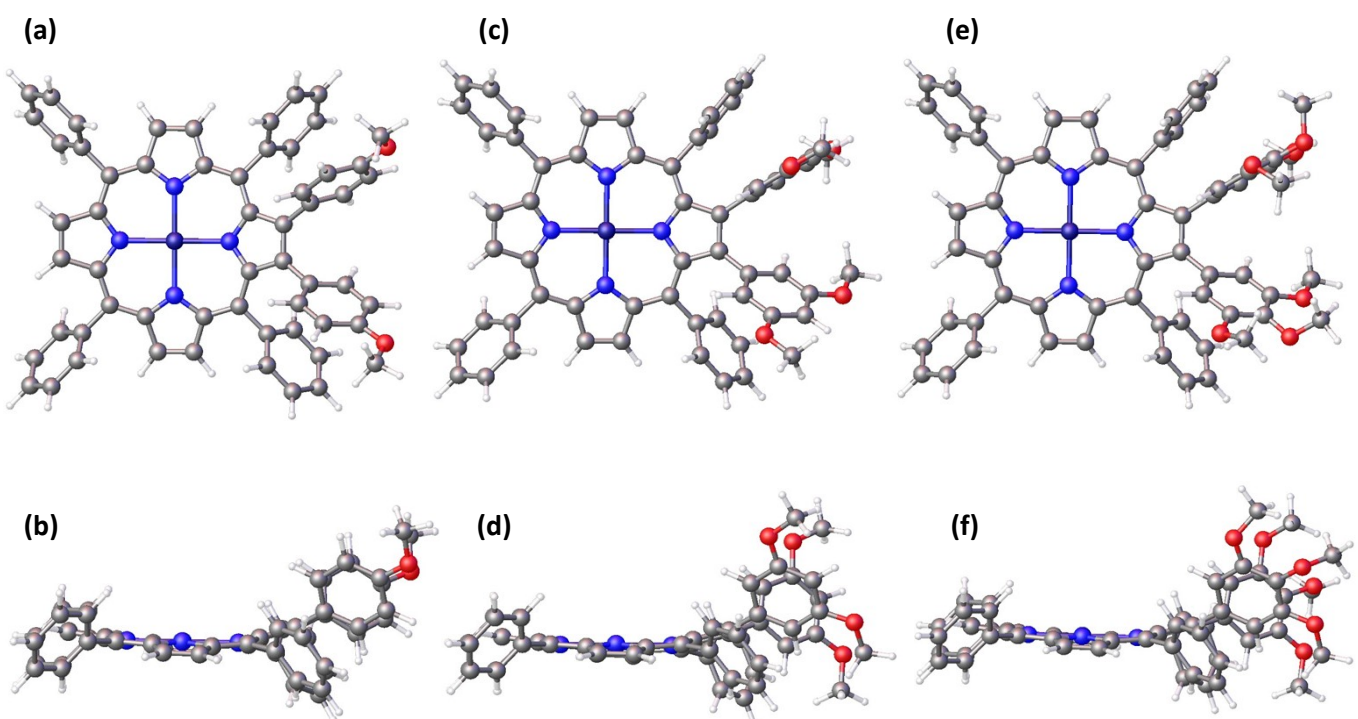


Figure S14. B3LYP/LanL2DZ optimized geometries showing top as well as side views of ZnTPP(*p*-CH₃O-Ph)₂ (a & b), ZnTPP(*m*-CH₃O-Ph)₂ (c & d) and ZnTPP(*m,p*-CH₃O-Ph)₂ (e & f).

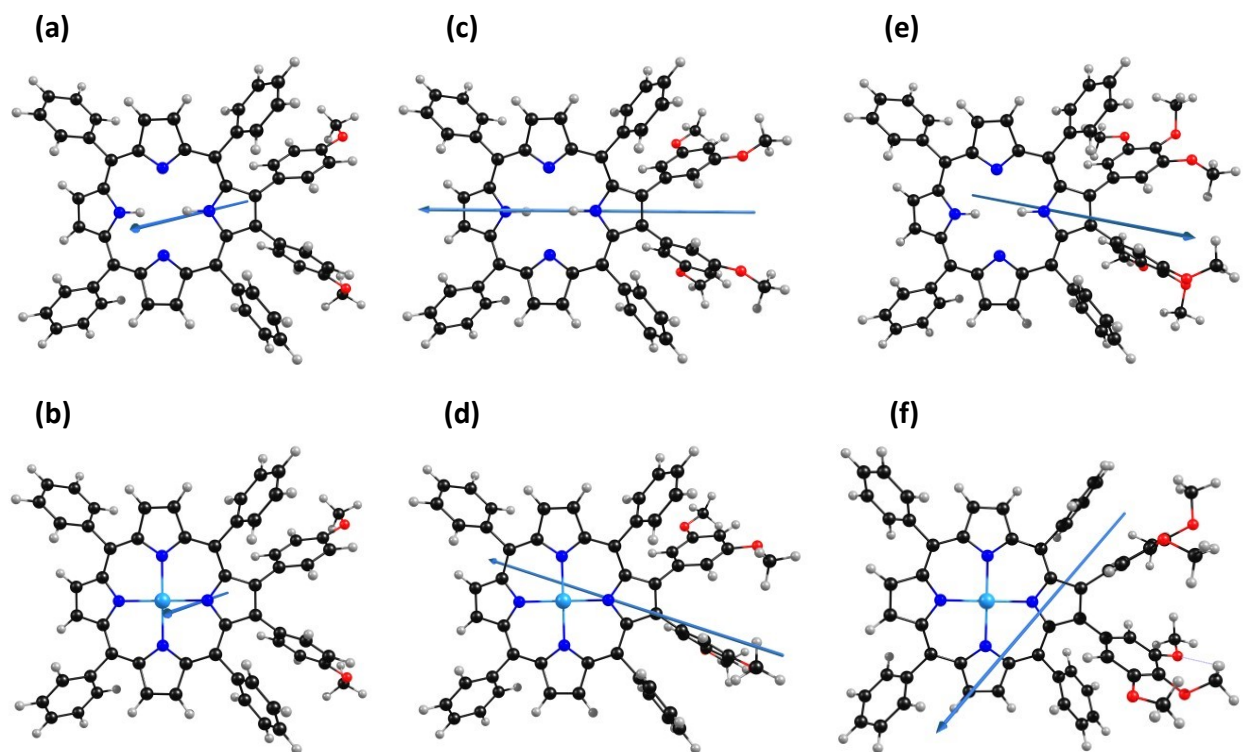


Figure S15. B3LYP/6-31G optimized geometries showing direction of dipole moment of MTPP(*p*-CH₃O-Ph)₂, M = 2H, Zn (a, b), MTPP(*m*-CH₃O-Ph)₂, M = 2H, Zn (c, d) & MTPP(*m,p*-CH₃O-Ph)₂, M = 2H, Zn (e, f) respectively. by using B3LYP-6-31G (d, p) level of theory in combination with LANL2DZ basis set Color codes for atoms: C (black), N (blue), H (white) and O (red) and Zn (light blue).

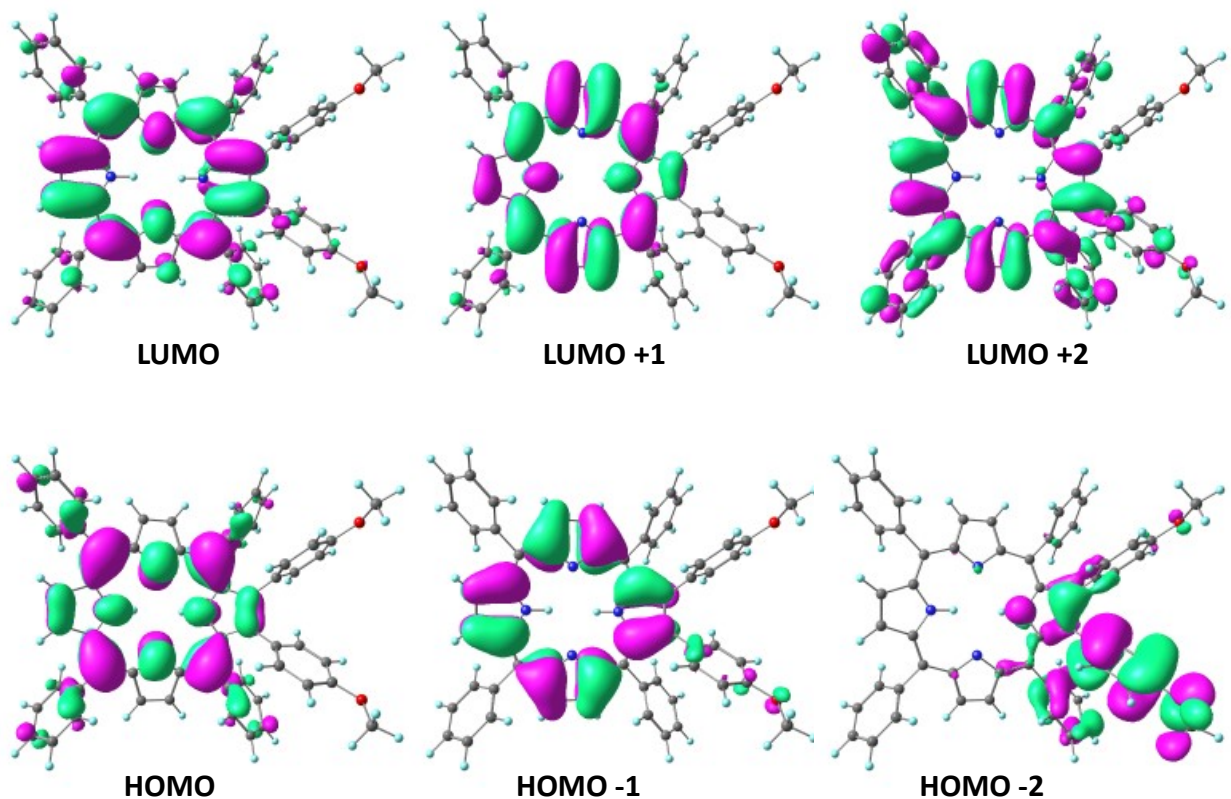


Figure S16. B3LYP/6-31G optimized geometries showing Frontier Molecular Orbitals (FMOs) of $\text{H}_2\text{TPP}(p\text{-CH}_3\text{O}\text{-Ph})_2$ respectively (having isosurface contour value of 0.03).

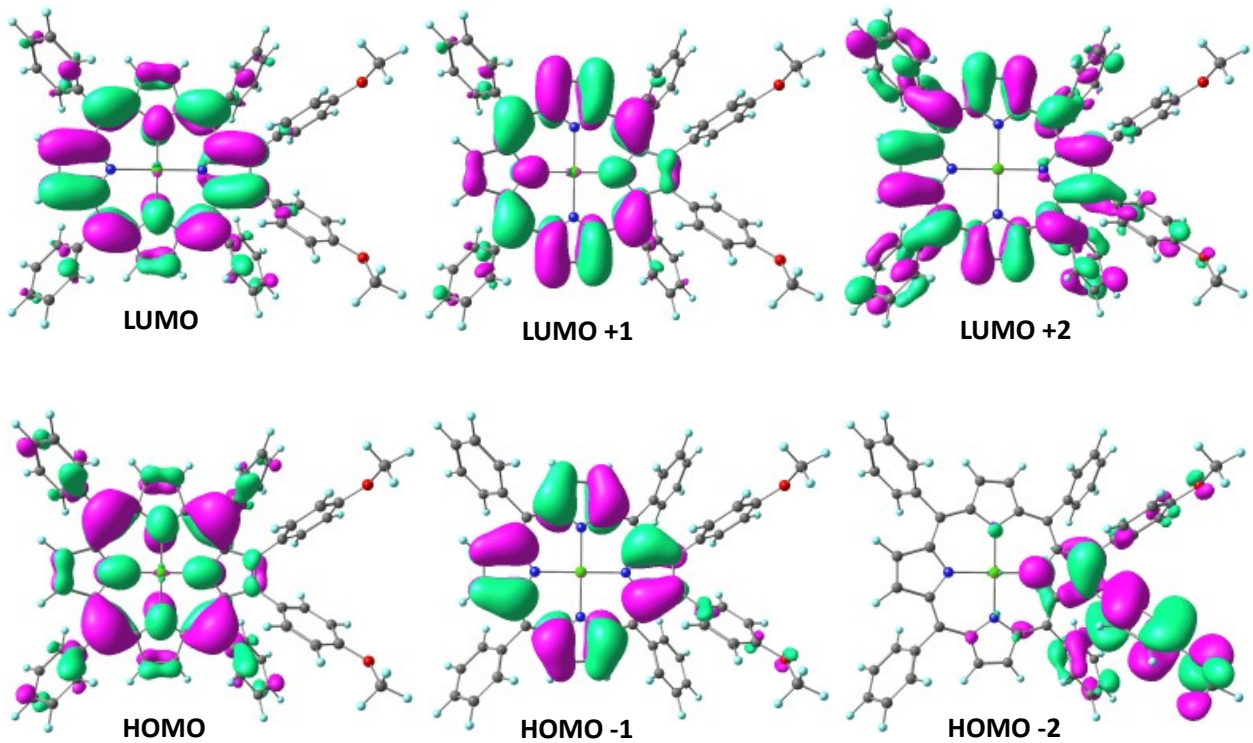


Figure S17. B3LYP/6-31G optimized geometries showing Frontier Molecular Orbitals (FMOs) of $\text{ZnTPP}(p\text{-CH}_3\text{O}\text{-Ph})_2$ respectively (having isosurface contour value of 0.03).

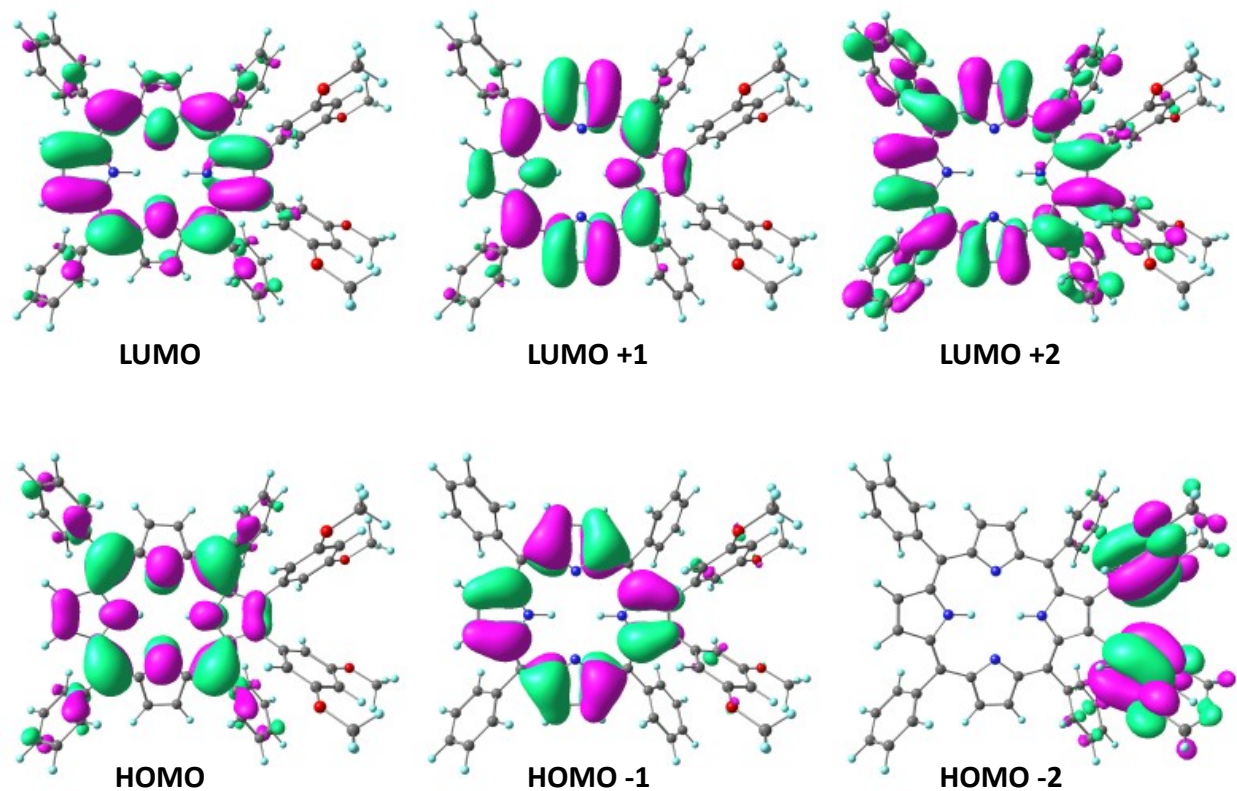


Figure S18. B3LYP/6-31G optimized geometries showing Frontier Molecular Orbitals (FMOs) of $\text{H}_2\text{TPP}(m\text{-CH}_3\text{O}\text{-Ph})_2$ respectively (having isosurface contour value of 0.03).

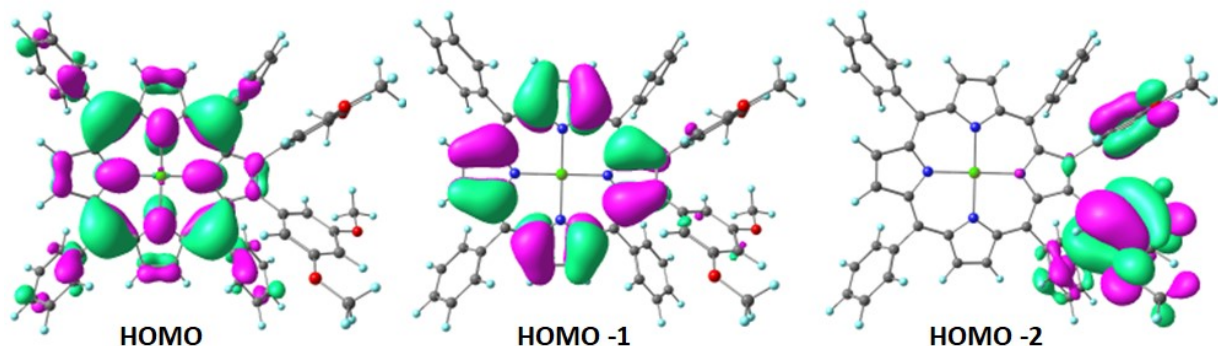
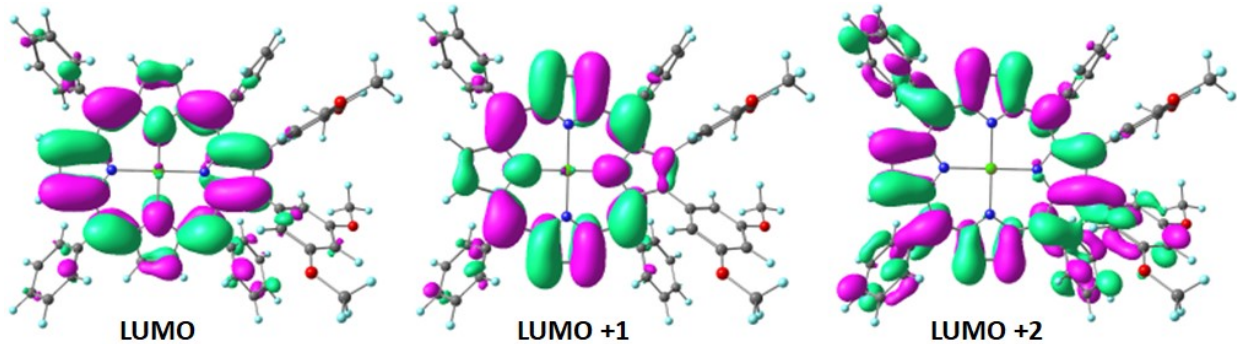


Figure S19. B3LYP/6-31G optimized geometries showing Frontier Molecular Orbitals (FMOs) of $\text{H}_2\text{TPP}(m\text{-CH}_3\text{O}\text{-Ph})_2$ respectively (having isosurface contour value of 0.03).

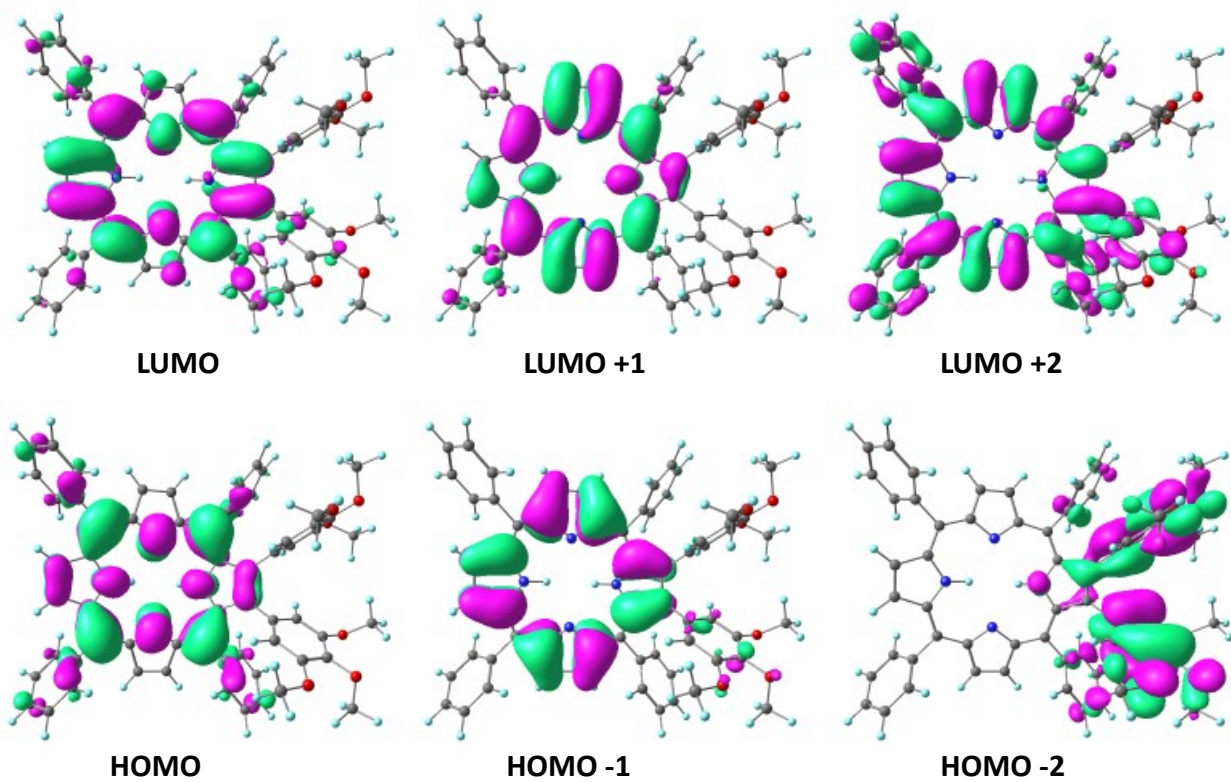


Figure S20. B3LYP/6-31G optimized geometries showing Frontier Molecular Orbitals (FMOs) of $\text{H}_2\text{TPP}(m,p\text{-CH}_3\text{O-Ph})_2$ respectively (having isosurface contour value of 0.03).

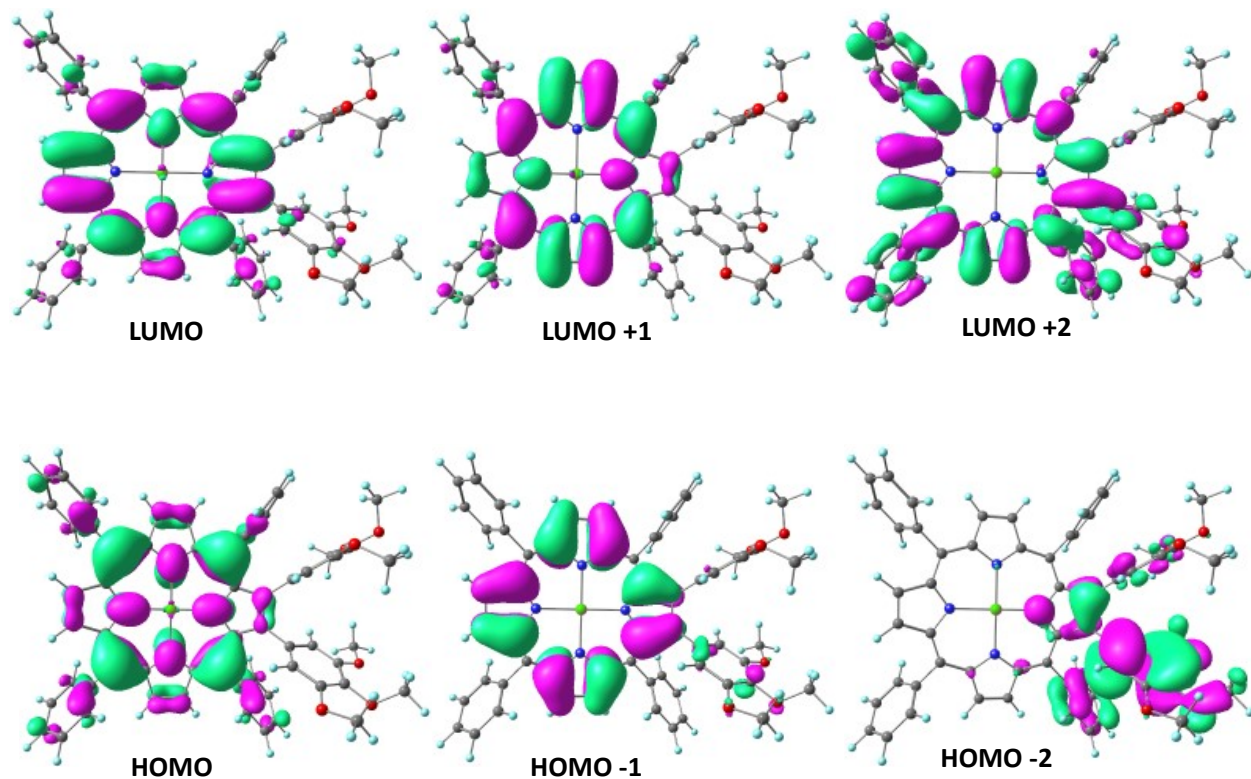


Figure S21. B3LYP/6-31G optimized geometries showing Frontier Molecular Orbitals (FMOs) of $\text{ZnTPP}(m,p\text{-CH}_3\text{O-Ph})_2$ respectively (having isosurface contour value of 0.03).

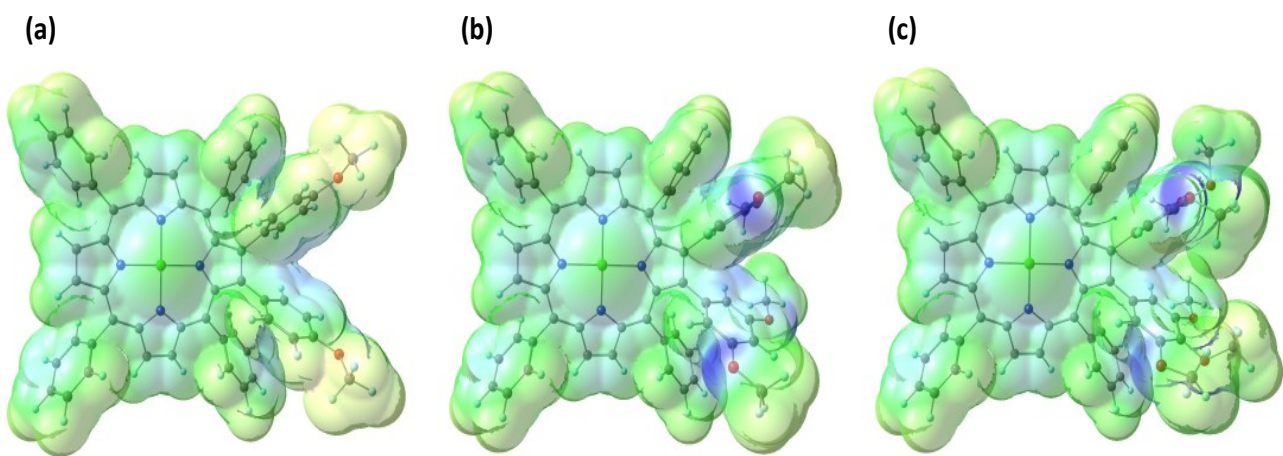


Figure S22. Molecular electrostatic potential (MEP) Zinc porphyrins:(a) $\text{ZnTPP}(p\text{-CH}_3\text{O-Ph})_2$ (b) $\text{ZnTPP}(m\text{-CH}_3\text{O-Ph})_2$ and (c) $\text{ZnTPP}(m,p\text{-CH}_3\text{O-Ph})_2$ using the B3LYP/ 6 31G (d, p) technique in the Gaussian 16W, in gas phase.

Table S8. The calculated Absorption, Oscillator strength, Molecular Transitions (M.T.), % weight contribution (% Ci > 10) of synthesized [ZnTPP(R)₂ R = *p*-CH₃O-Ph, *m*-CH₃O-Ph & *m,p*-CH₃O-Ph] at B3LYP-6-31G (d, p) level of theory in combination with LANL2DZ basis set.

Compounds	State	Molecular transitions (M.T.)	Excited state energy (eV)	Weight contribution (%Ci)	Calculated λ (nm) in DCM	Oscillatory strength (f)	Experimental λ (nm) in DCM
ZnTPP(<i>p</i> -CH ₃ O-Ph) ₂	S1	H-1 → L +1	2.1826 eV	30	568	0.0753	589
		H → L		69			
	S2	H-1 → L	2.2076 eV	37	562	0.0261	553
		H → L +1		62			
	S3	H-2 → L	2.7977 eV	79	443	0.1741	486
	S4	H-3 → L	2.9252 eV	89	424	0.0382	425
	S5	H-3 → L +1	2.9348 eV	61	422	0.4469	
		H-2 → L		14			
		H-2 → L+1		10			
ZnTPP(<i>m</i> -CH ₃ O-Ph) ₂	S1	H-1 → L +1	2.1963eV	31	565	0.0658	594
		H → L		68			
	S2	H-1 → L	2.2196 eV	39	559	0.0192	552
		H → L +1		61			
	S3	H-2 → L	2.7832 eV	97	446	0.004	487
	S4	H-3 → L	2.9038 eV	19	427	0.021	
		H-2 → L+1		79			423
	S5	H-3 → L	2.9227 eV	51	424	0.4361	
		H-2 → L+1		18			
		H-1 → L		16			
ZnTPP(<i>m,p</i> -CH ₃ O-Ph) ₂	S1	H-1 → L +1	2.2021 eV	32	563	0.0605	592
		H → L		68			
	S2	H-1 → L	2.236 eV	39	558	0.0168	551
		H → L +1		60			
	S3	H-2 → L	2.8053 eV	85	442	0.1536	486
	S4	H-2 → L+1		77		0.1641	
	S5	H-3 → L	2.9384 eV	89	419	0.0138	422

Figure S23. ^1H NMR spectrum of $\text{H}_2\text{TPP}(p\text{-CH}_3\text{O-Ph})_2$ in CDCl_3 at 298 K.

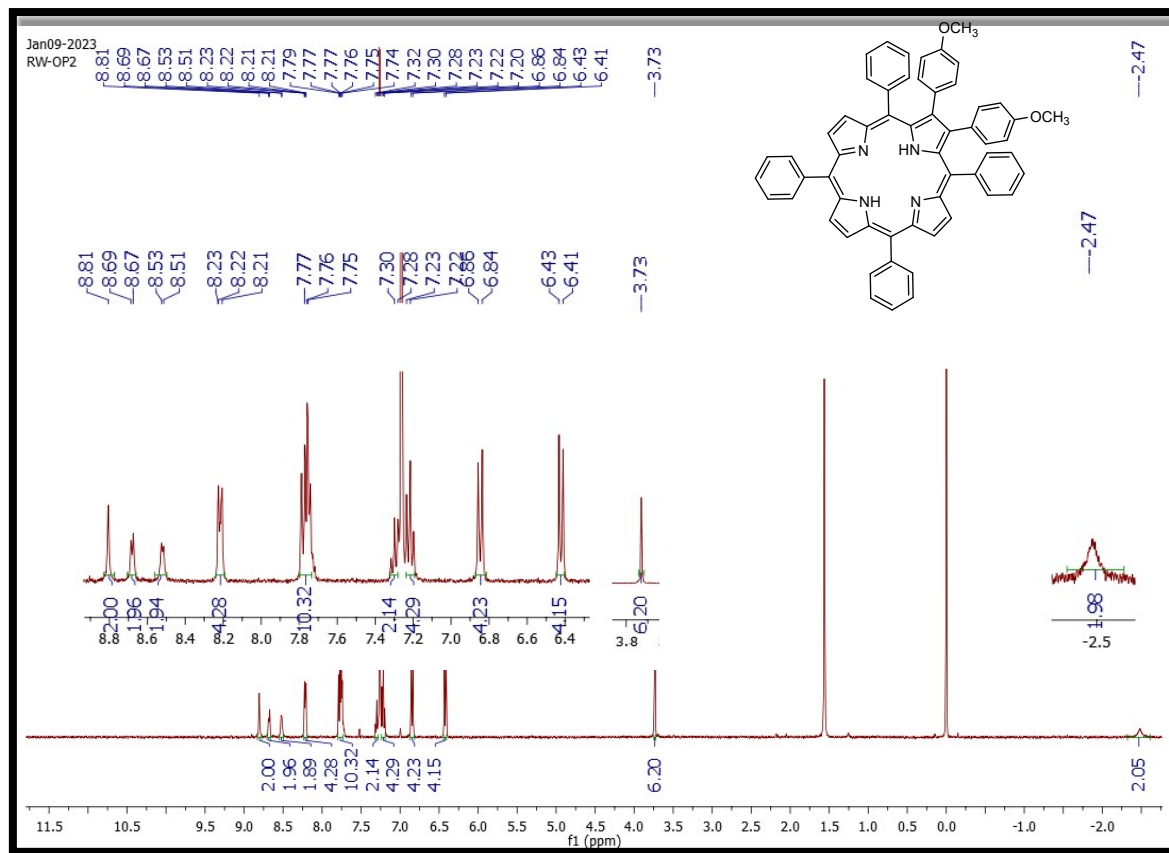


Figure S24. ^1H NMR spectrum of ZnTPP(*p*-CH₃O-Ph)₂ in CDCl₃ at 298 K.

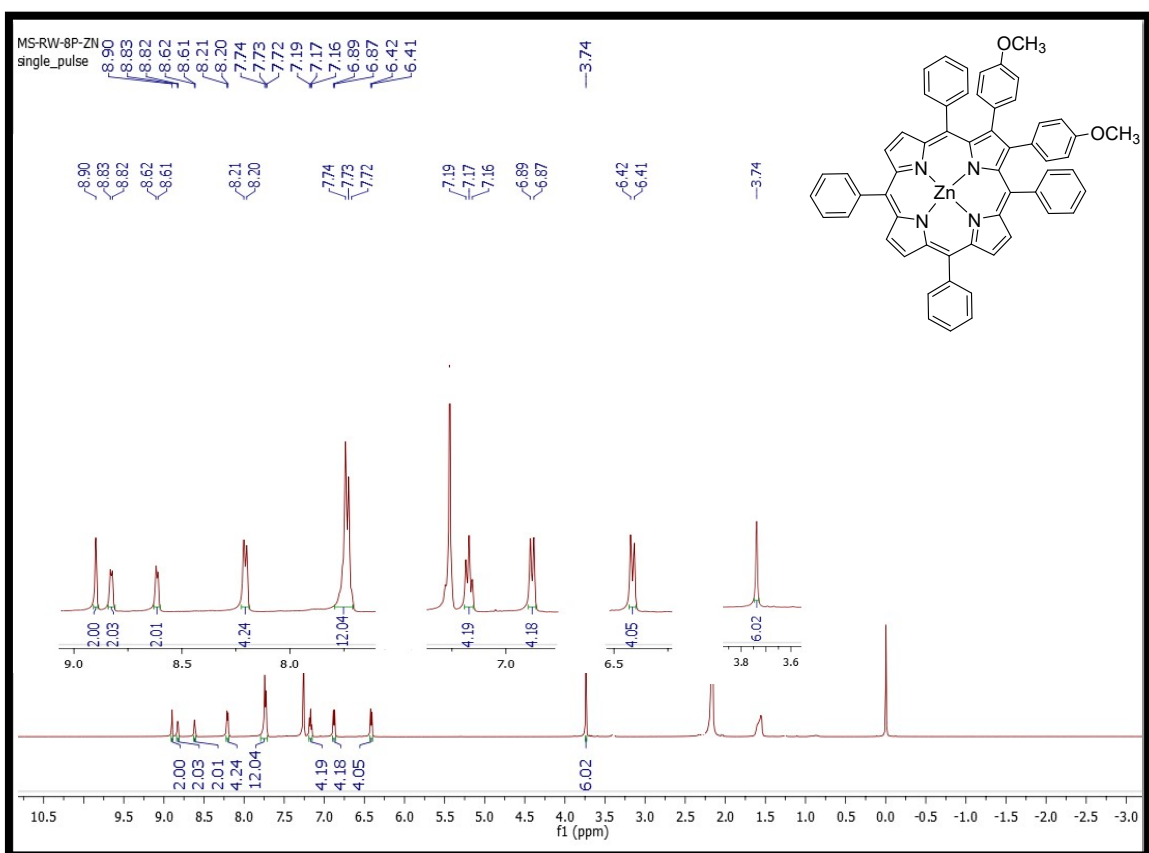


Figure S25. ^1H NMR spectrum of NiTPP(*p*-CH₃O-Ph)₂ in CDCl₃ at 298 K.

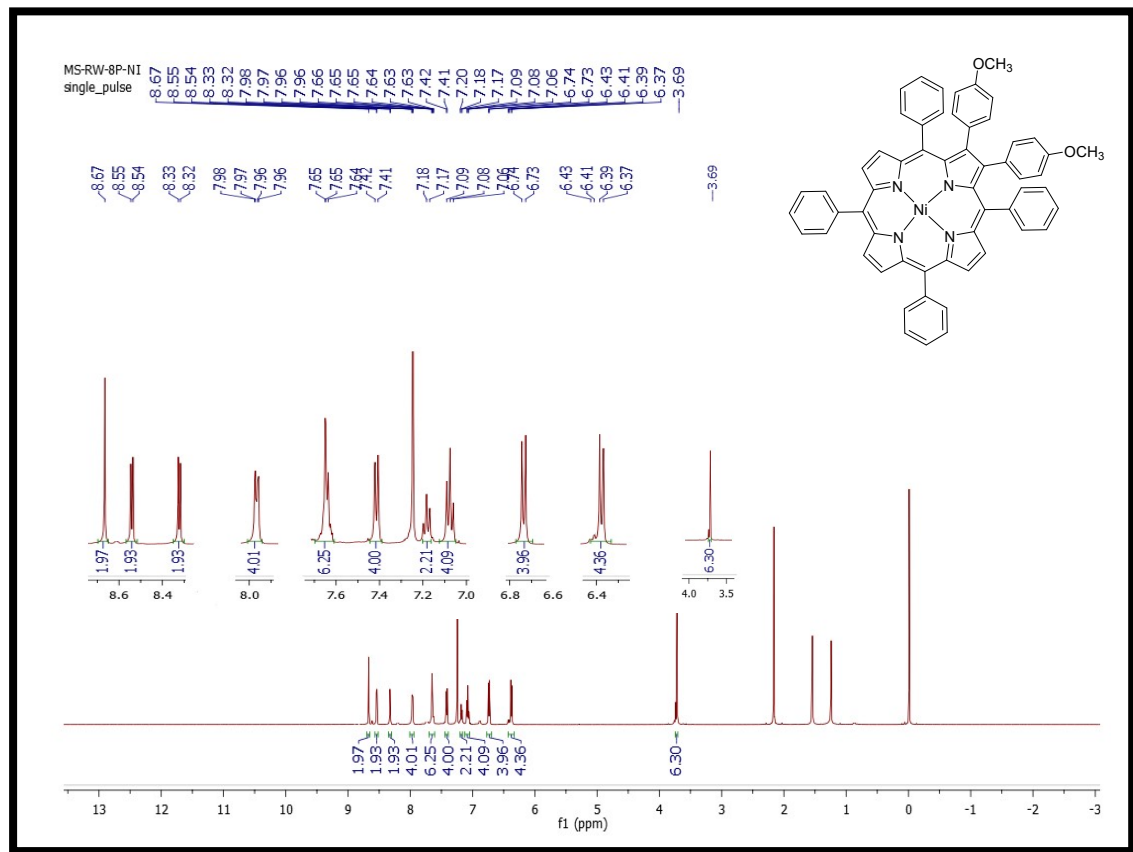


Figure S26. ^1H NMR spectrum of $\text{H}_2\text{TPP}(m\text{-CH}_3\text{O-Ph})_2$ in CDCl_3 at 298 K.

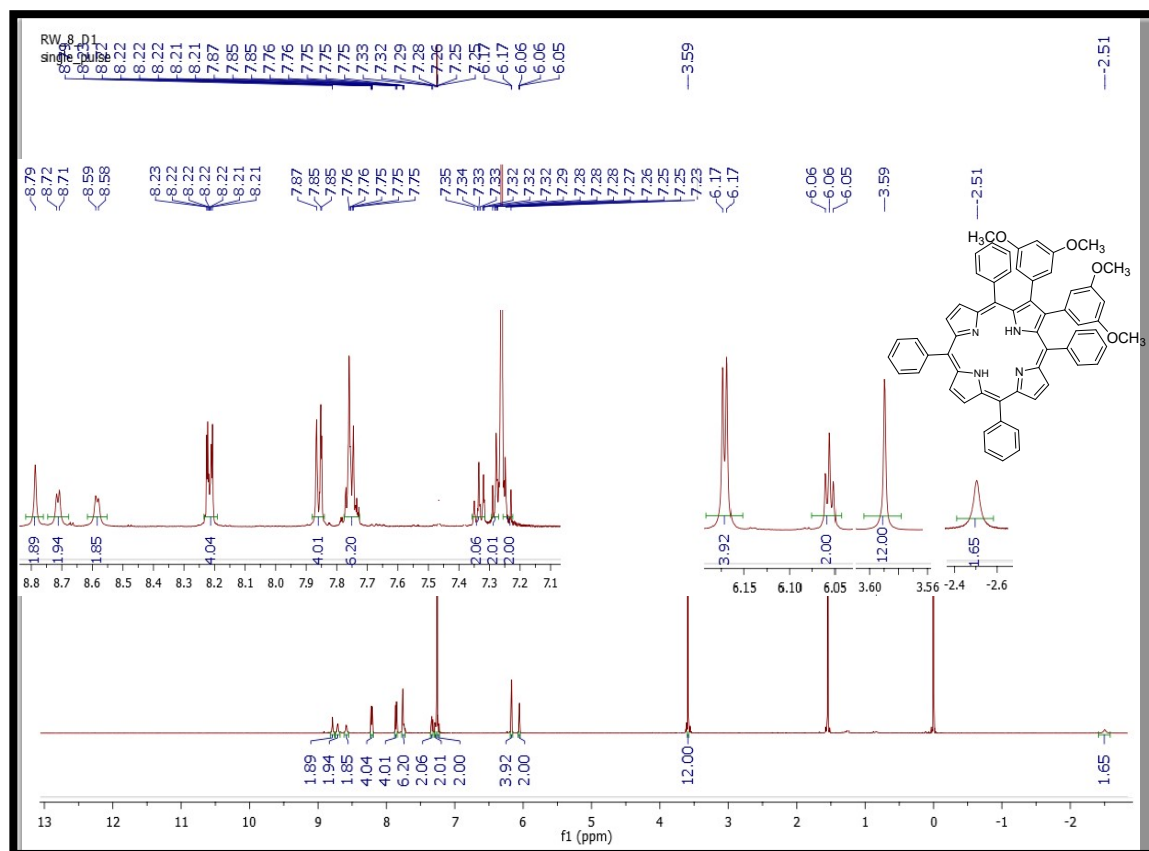


Figure S27. ^1H NMR spectrum of ZnTPP(*m*-CH₃O-Ph)₂ in CDCl₃ at 298 K.

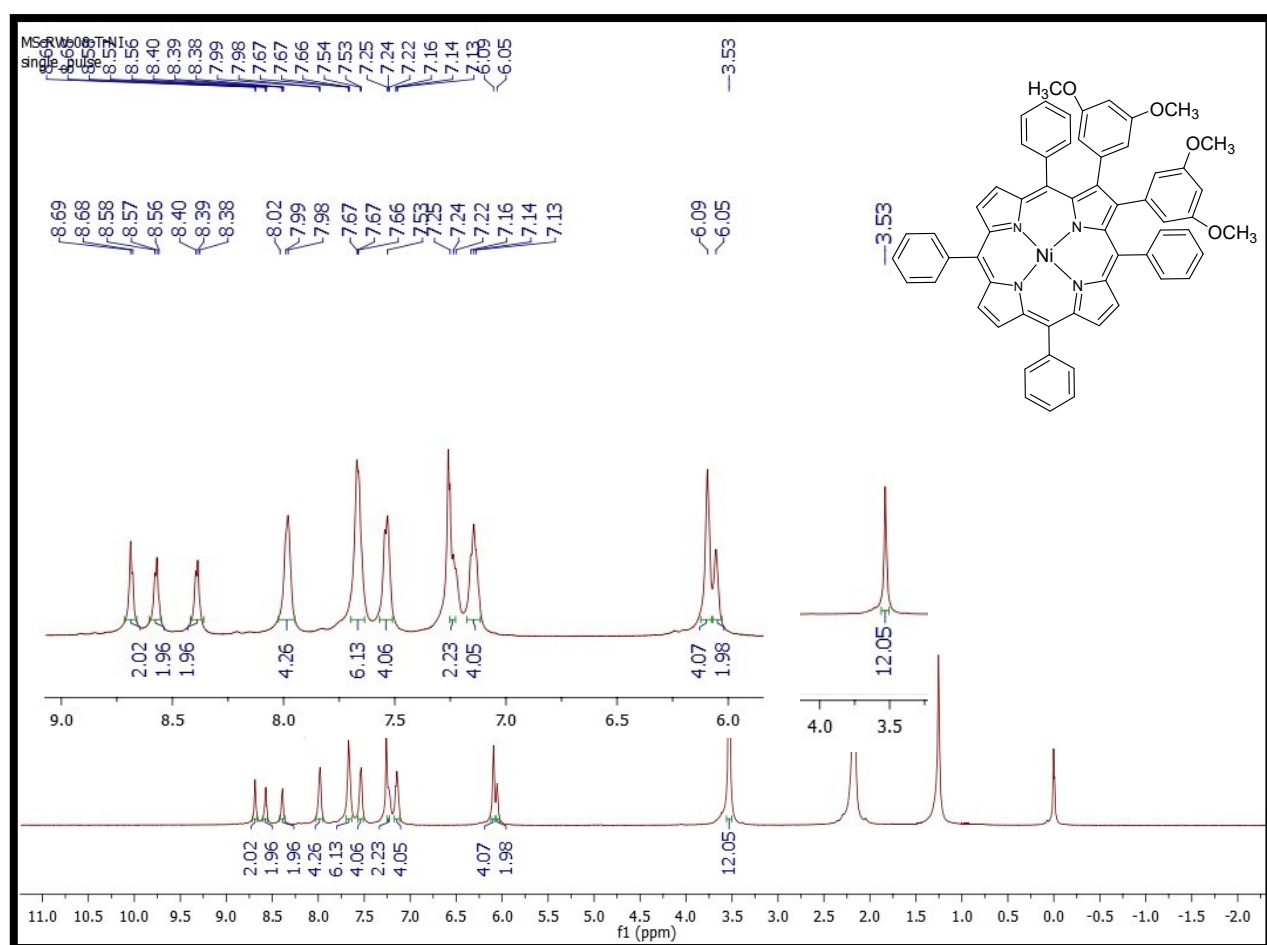
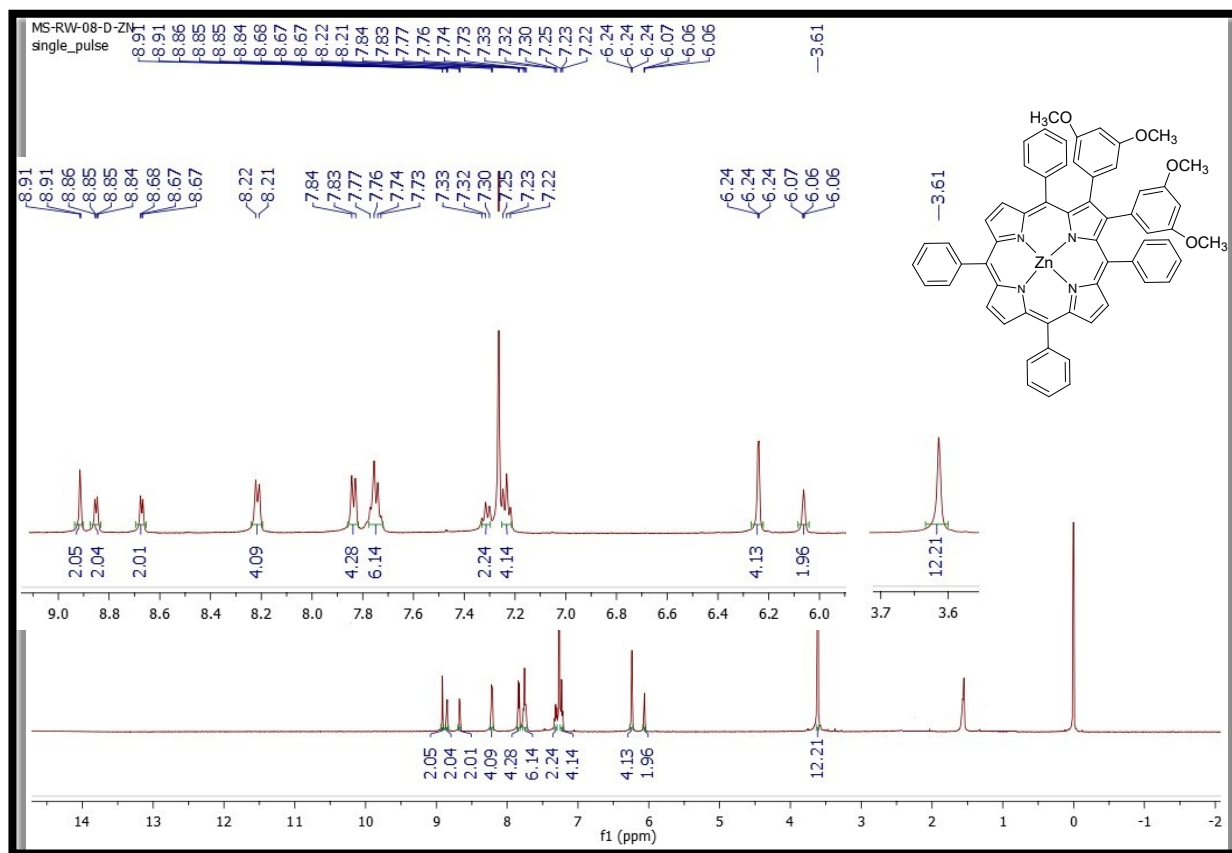


Figure S29. ^1H NMR spectrum of $\text{H}_2\text{TPP}(m,p\text{-CH}_3\text{O-Ph})_2$ in CDCl_3 at 298 K.

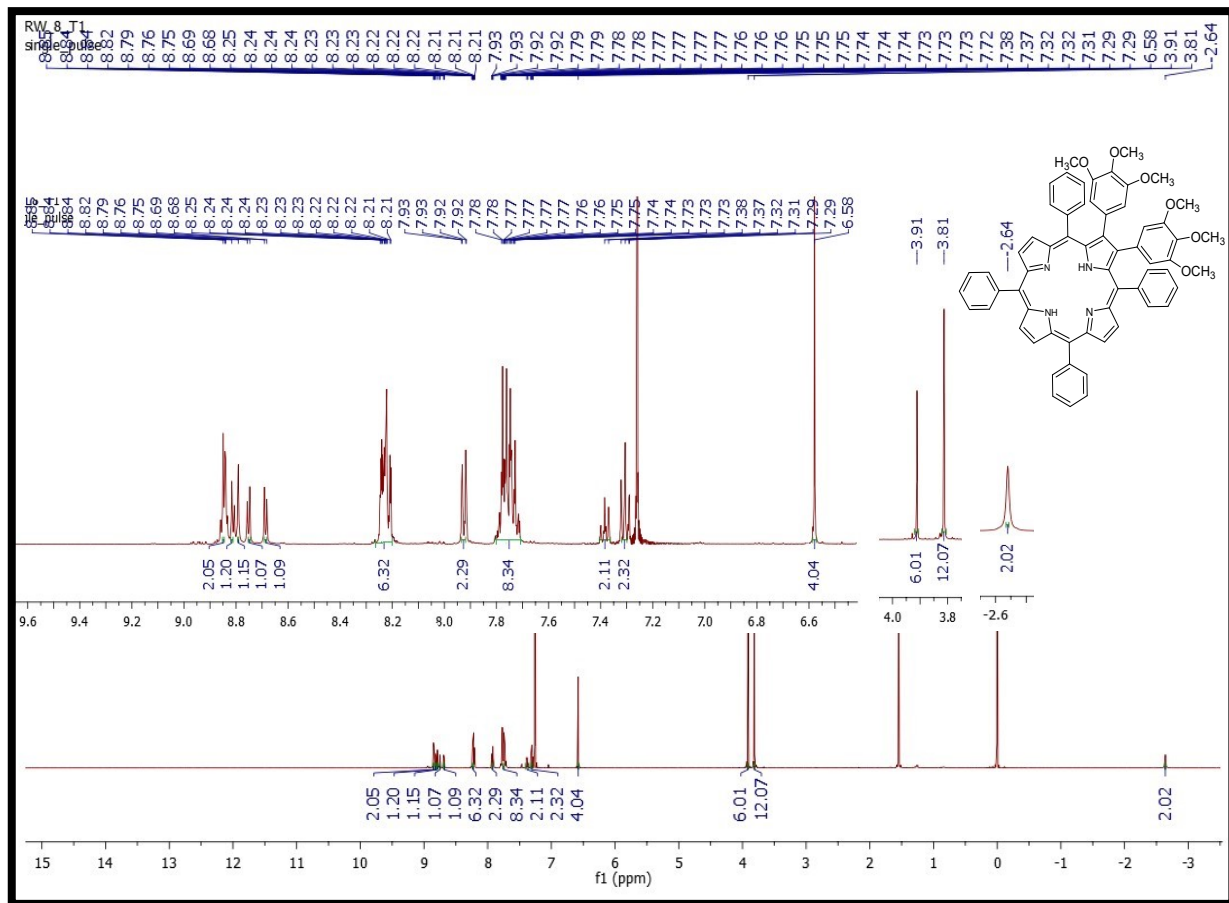


Figure S30. ^1H NMR spectrum of ZnTPP(*m,p*-CH₃O-Ph)₂ in CDCl₃ at 298 K.

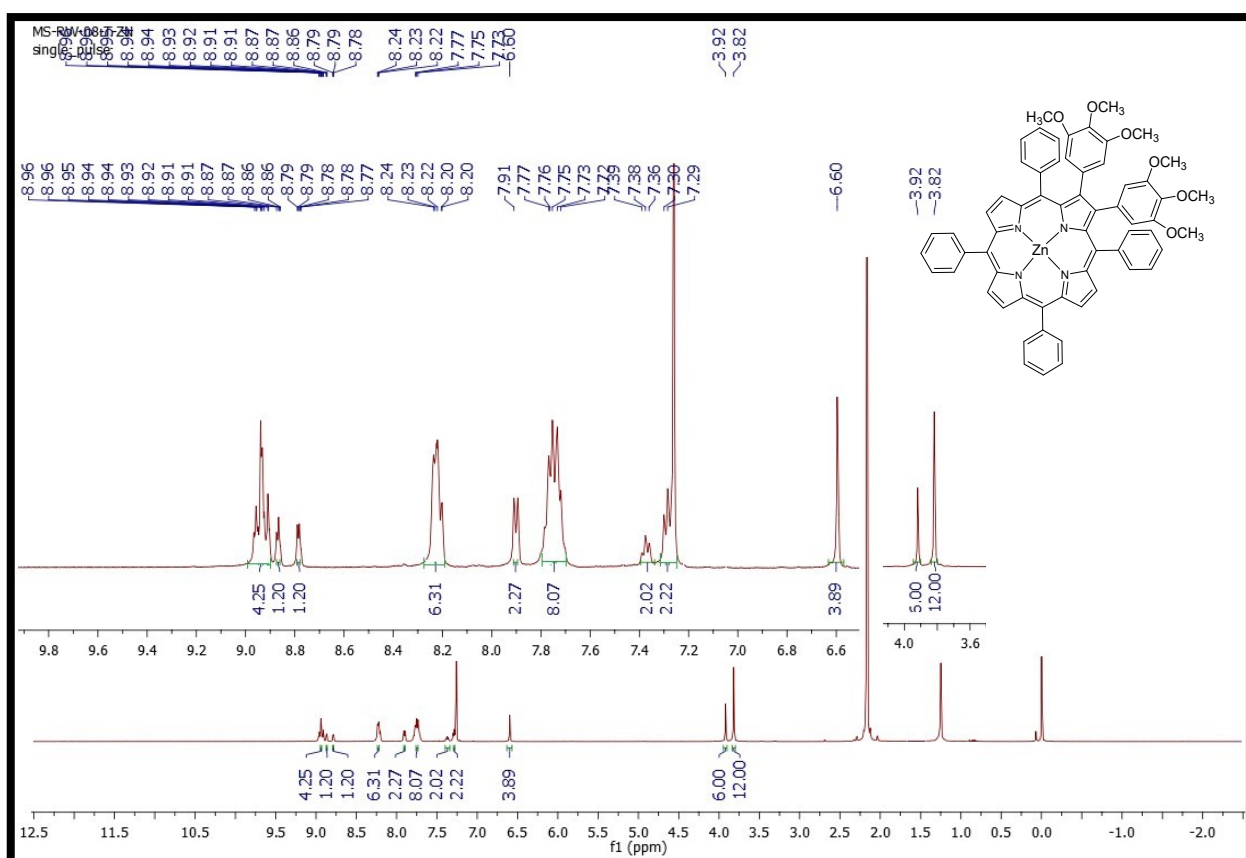


Figure S31. ^1H NMR spectrum of NiTPP(*m,p*-CH₃O-Ph)₂ in CDCl₃ at 298 K.

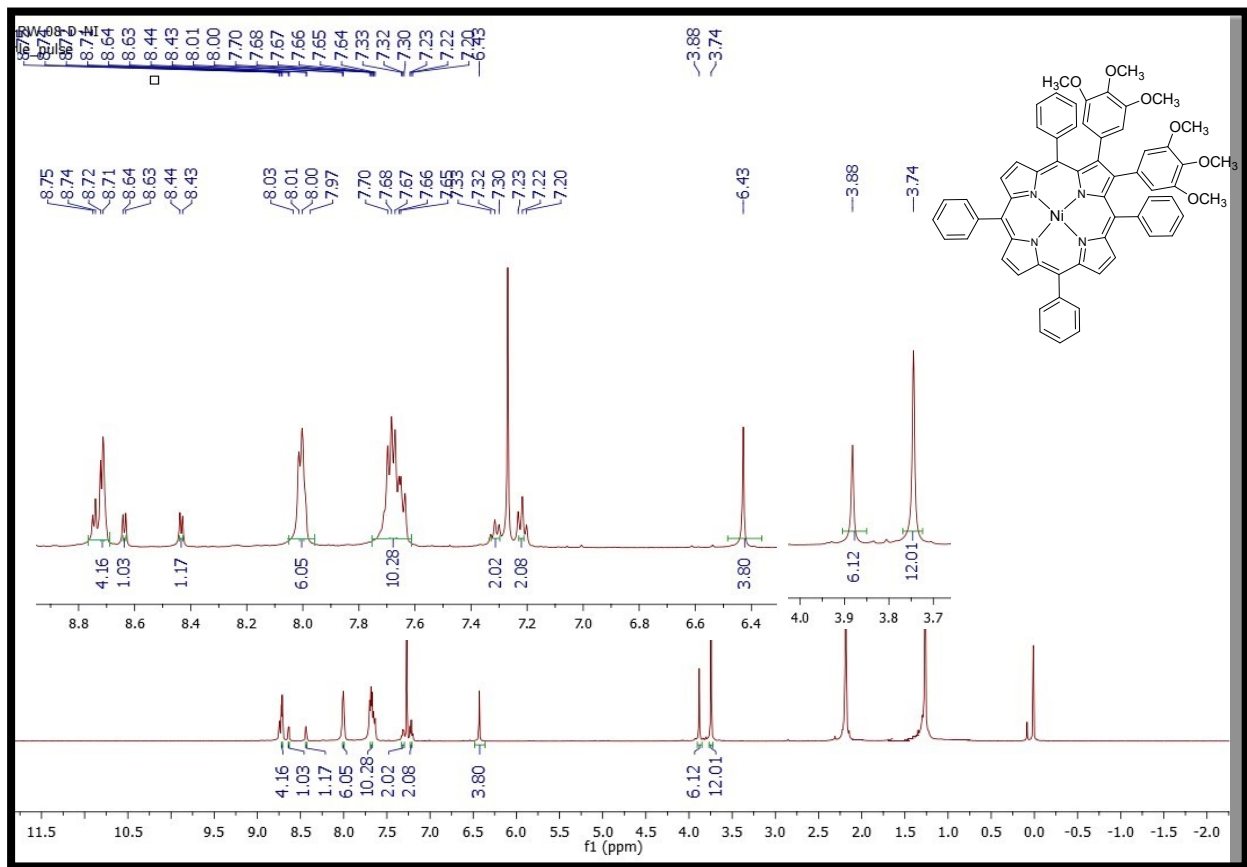


Figure S32. ^{13}C NMR spectrum of $\text{H}_2\text{TPP}(p\text{-CH}_3\text{O-Ph})_2$ in CDCl_3 at 298 K.

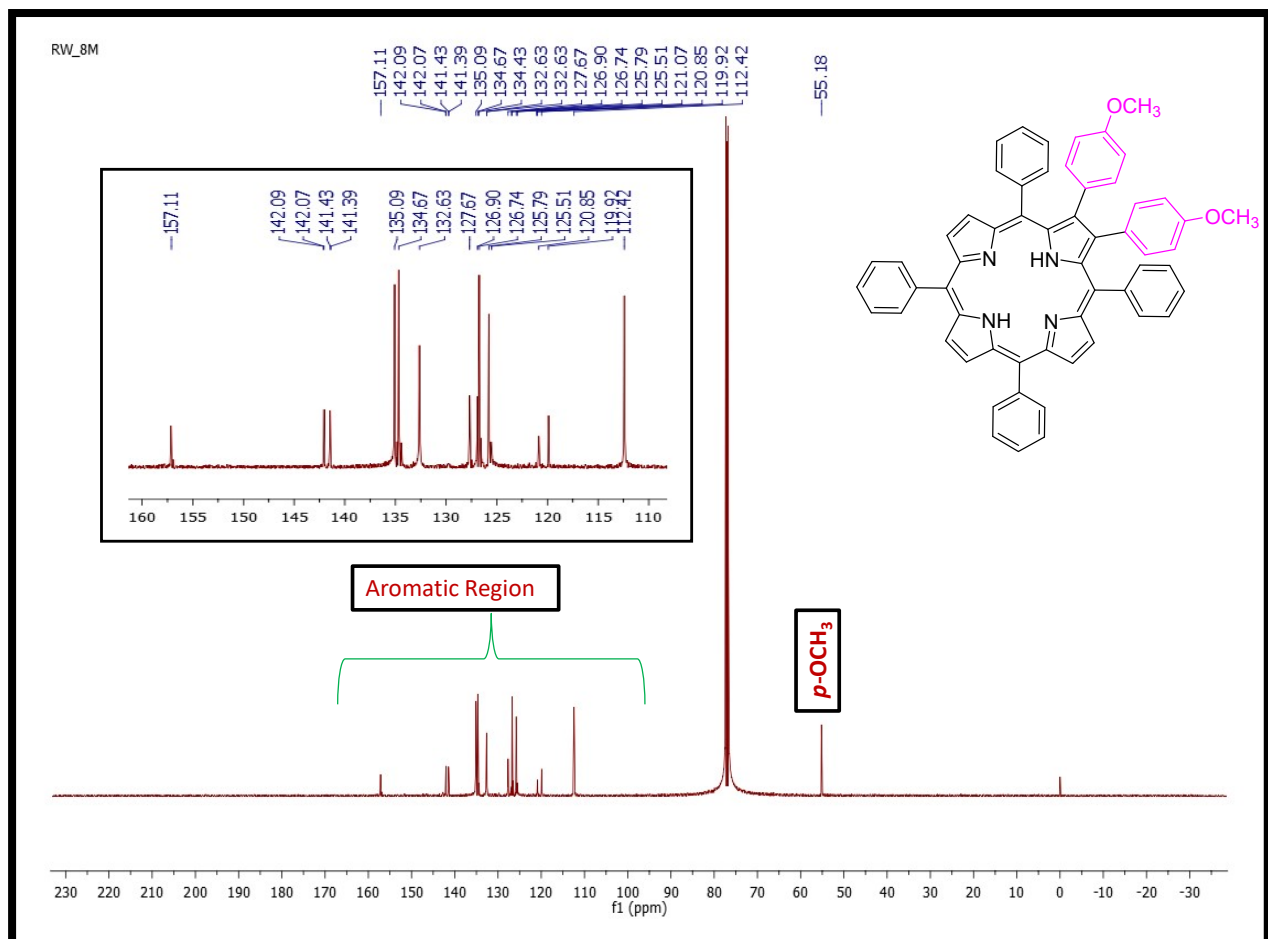


Figure S33. ^{13}C NMR spectrum of $\text{H}_2\text{TPP}(m\text{-CH}_3\text{O-Ph})_2$ in CDCl_3 at 298 K.

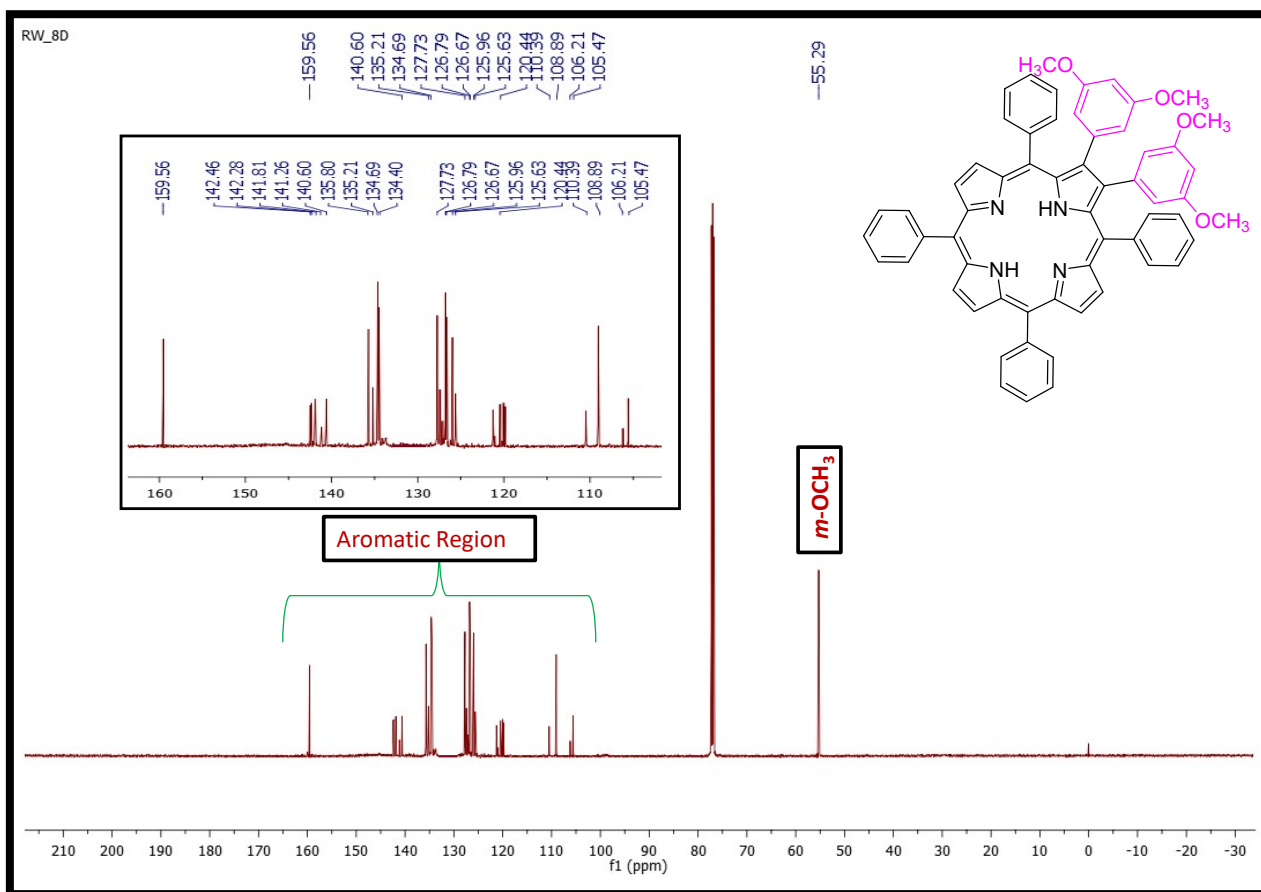
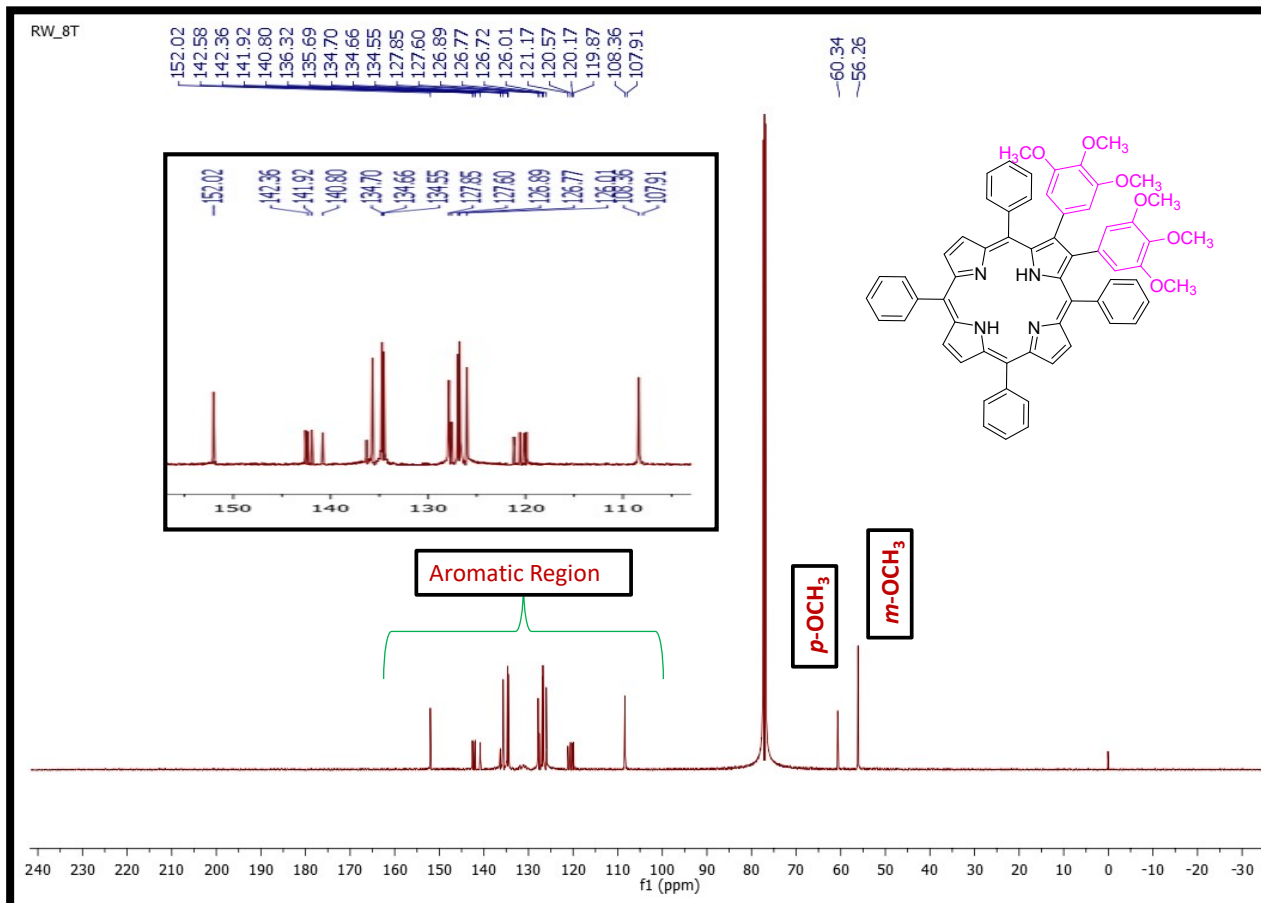


Figure S34. ^{13}C NMR spectrum of $\text{H}_2\text{TPP}(m,p\text{-CH}_3\text{O-Ph})_2$ in CDCl_3 at 298 K.



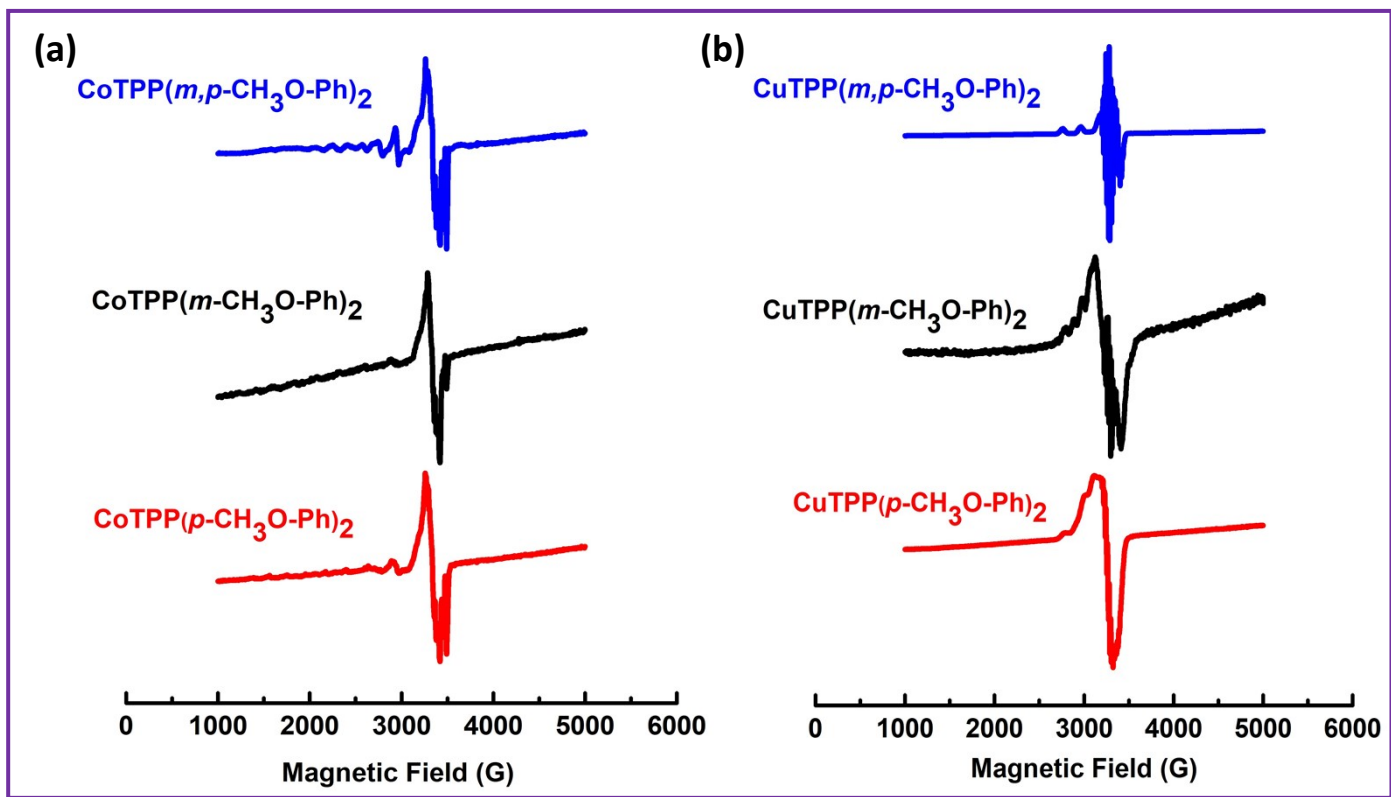


Figure S35. X-band EPR Spectra of (a) CoTPP(R)₂, where R = *p*-CH₃O-Ph, *m*-CH₃O-Ph & *m,p*-CH₃O-Ph (b) CuTPP(R)₂; where R = *p*-CH₃O-Ph, *m*-CH₃O-Ph & *m,p*-CH₃O-Ph in toluene at 100 K, with EPR parameters: microwave frequency 9.41 GHz, incident microwave power 1.7 mW, modulation frequency 100 kHz.

Figure S36. HRMS spectrum of H₂TPP(*p*-CH₃O-Ph)₂.

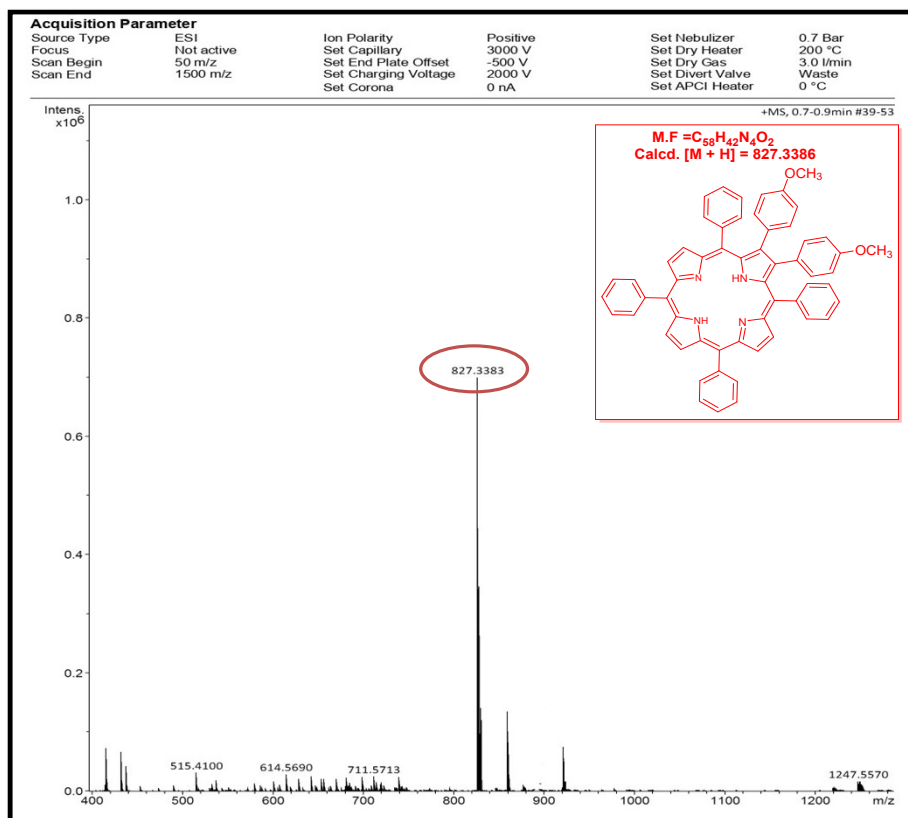


Figure S37. HRMS spectrum of ZnTPP(*p*-CH₃O-Ph)₂.

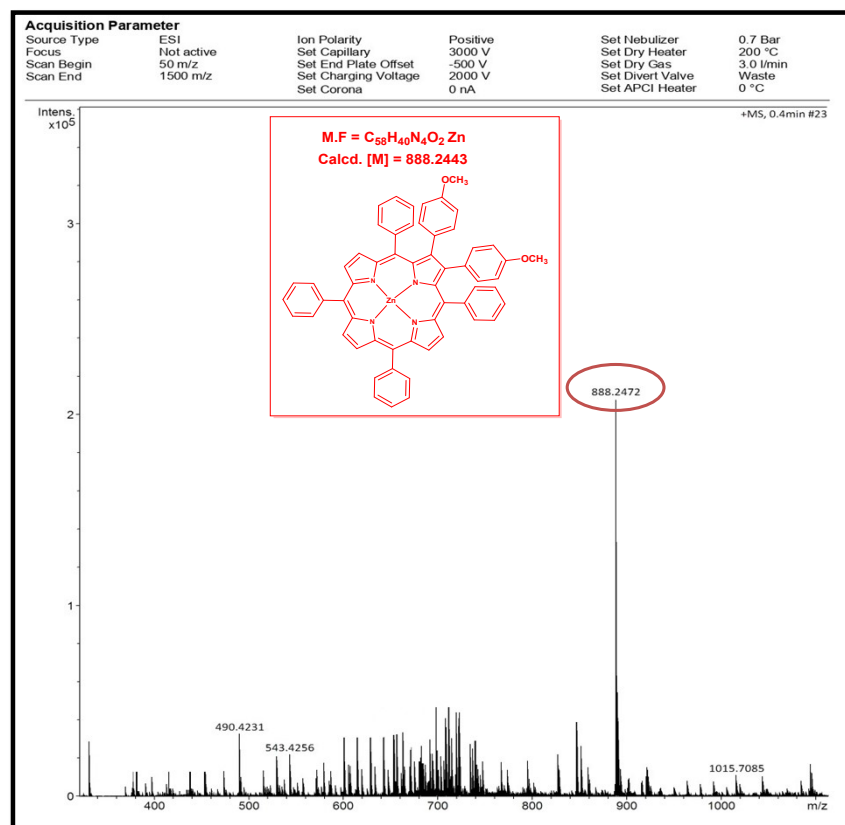


Figure S38. HRMS spectrum of NiTPP(*p*-CH₃O-Ph)₂.

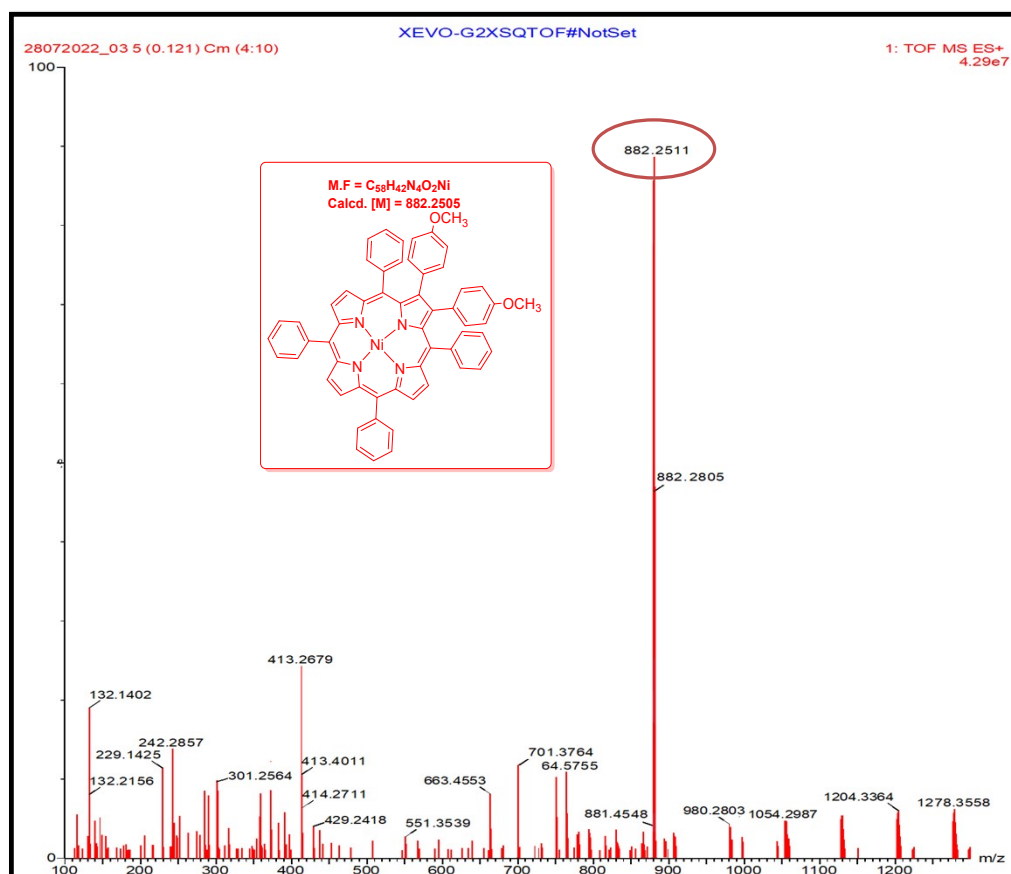


Figure S39. HRMS spectrum of CuTPP(*p*-CH₃O-Ph)₂.

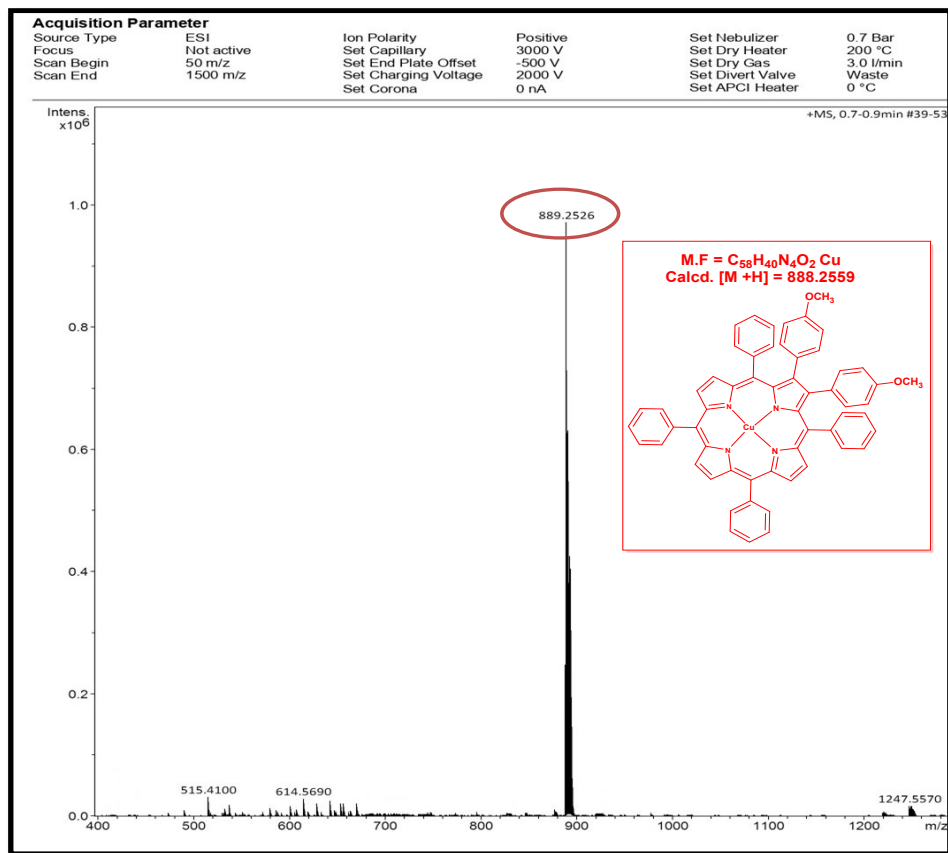


Figure S40. HRMS spectrum of CoTPP(*p*-CH₃O-Ph)₂.

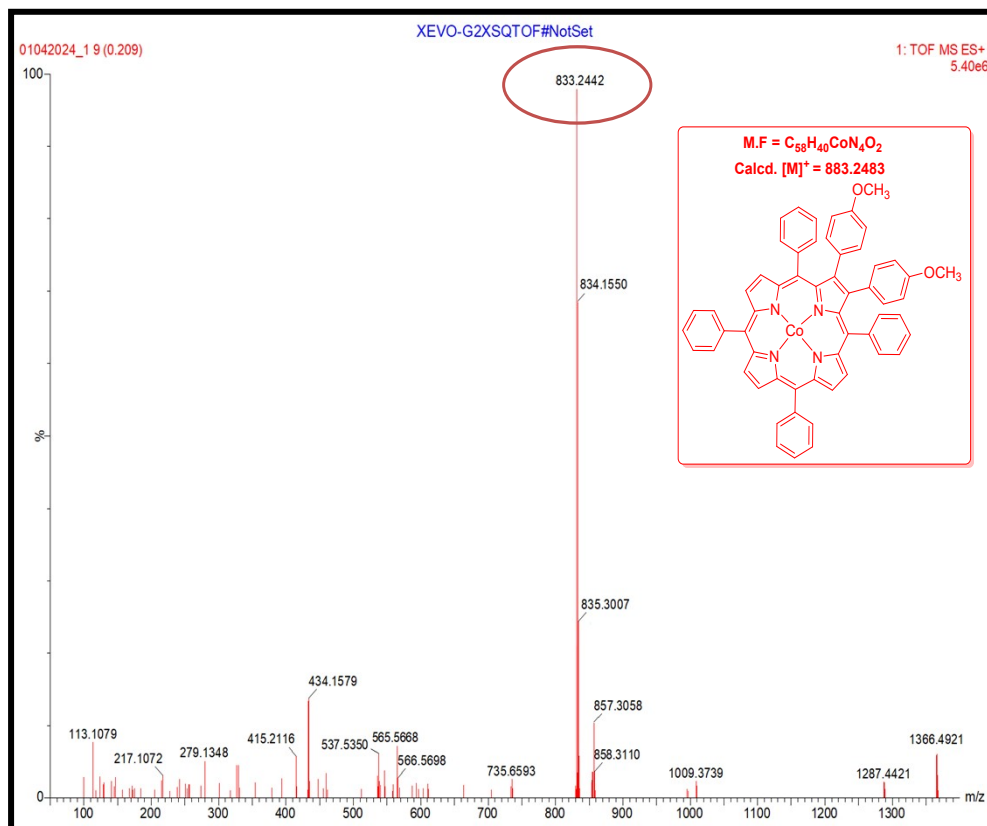


Figure S41. HRMS spectrum of H₂TPP(*m*-CH₃O-Ph)₂.

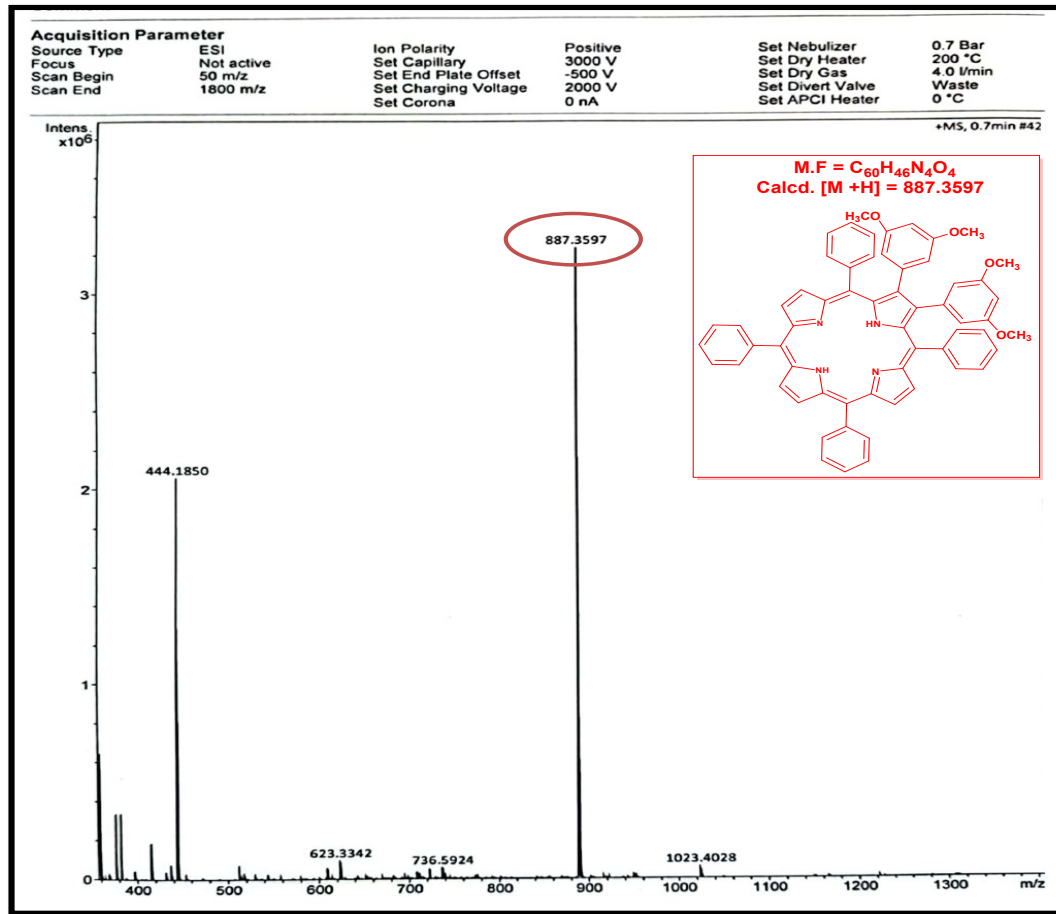


Figure S42. HRMS spectrum of ZnTPP(*m*-CH₃O-Ph)₂.

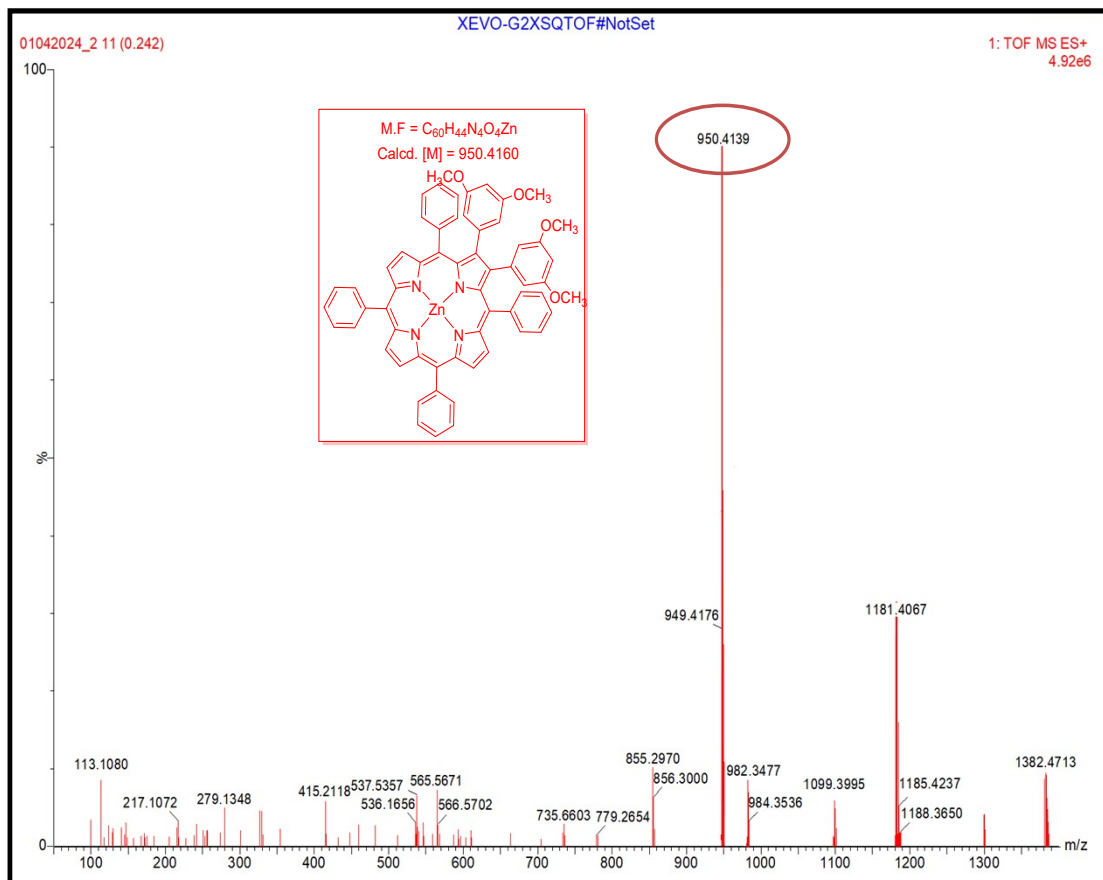


Figure S43. HRMS spectrum of NiTPP(*m*-CH₃O-Ph)₂.

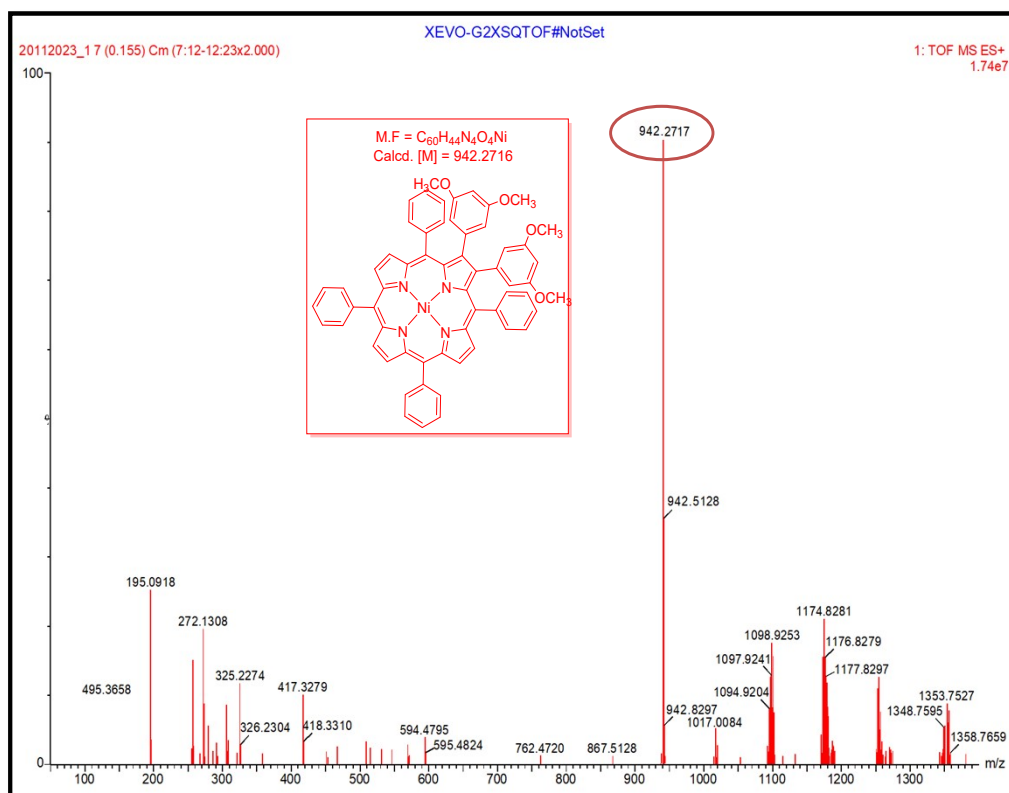


Figure S44. HRMS spectrum of CuTPP(*m*-CH₃O-Ph)₂.

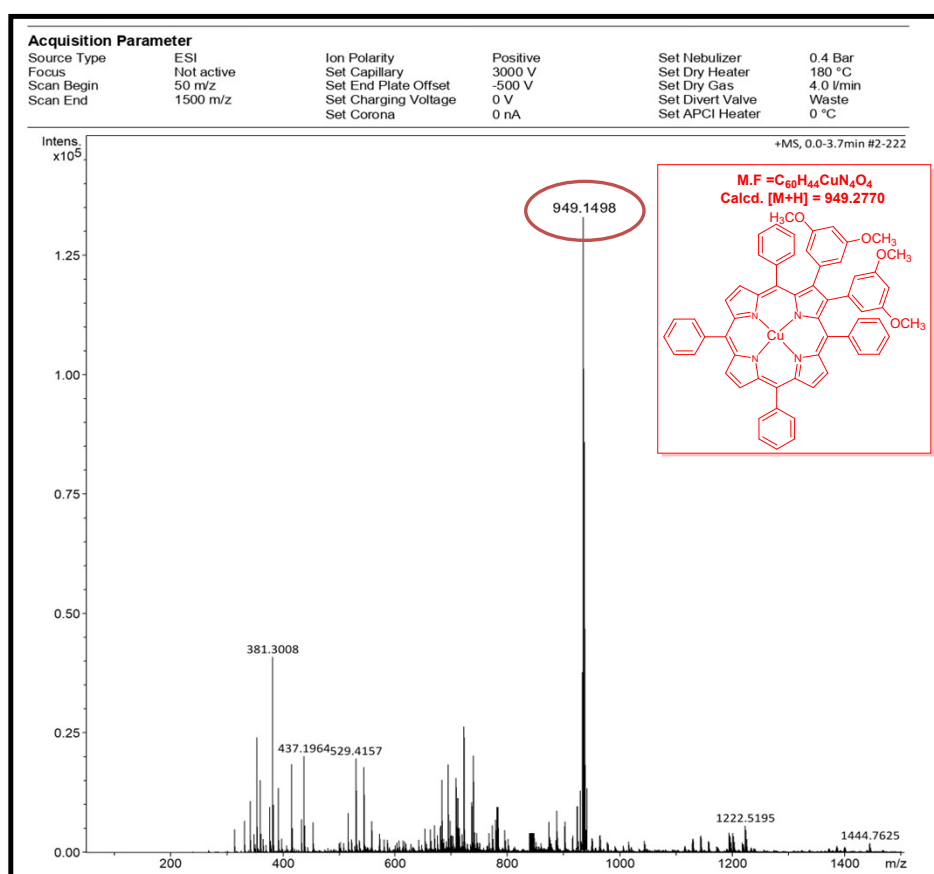


Figure S45. HRMS spectrum of CoTPP(*m*-CH₃O-Ph)₂.

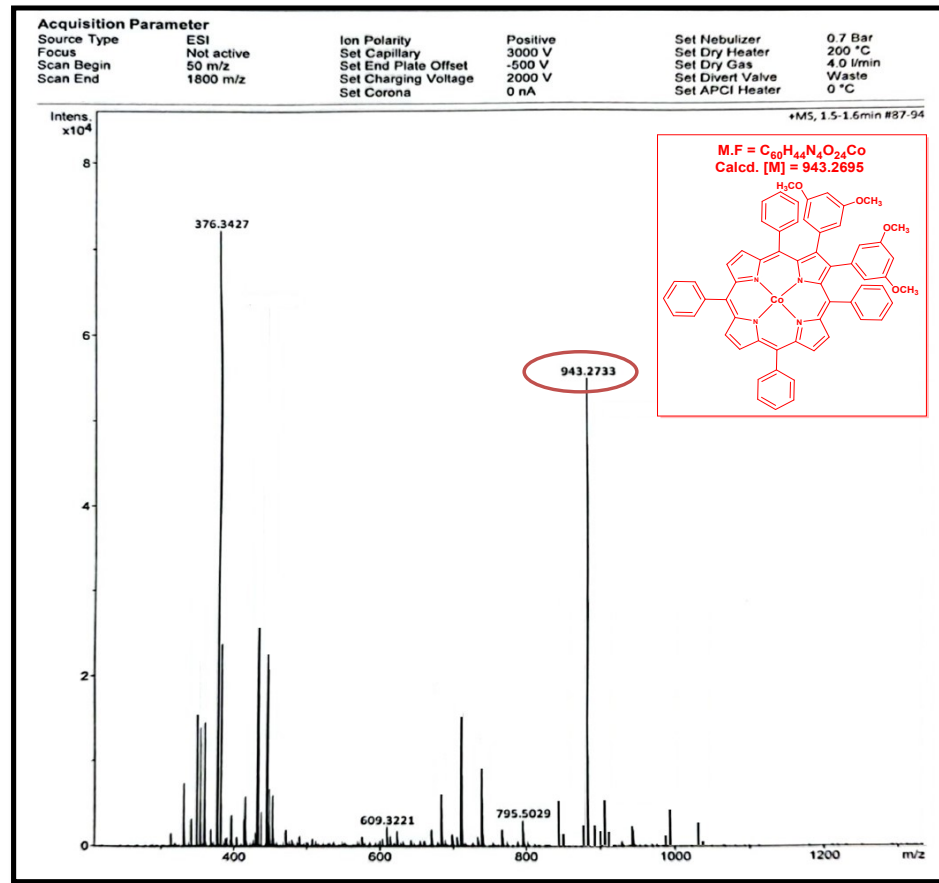


Figure S46. HRMS spectrum of H₂TPP(*m,p*-CH₃O-Ph)₂.

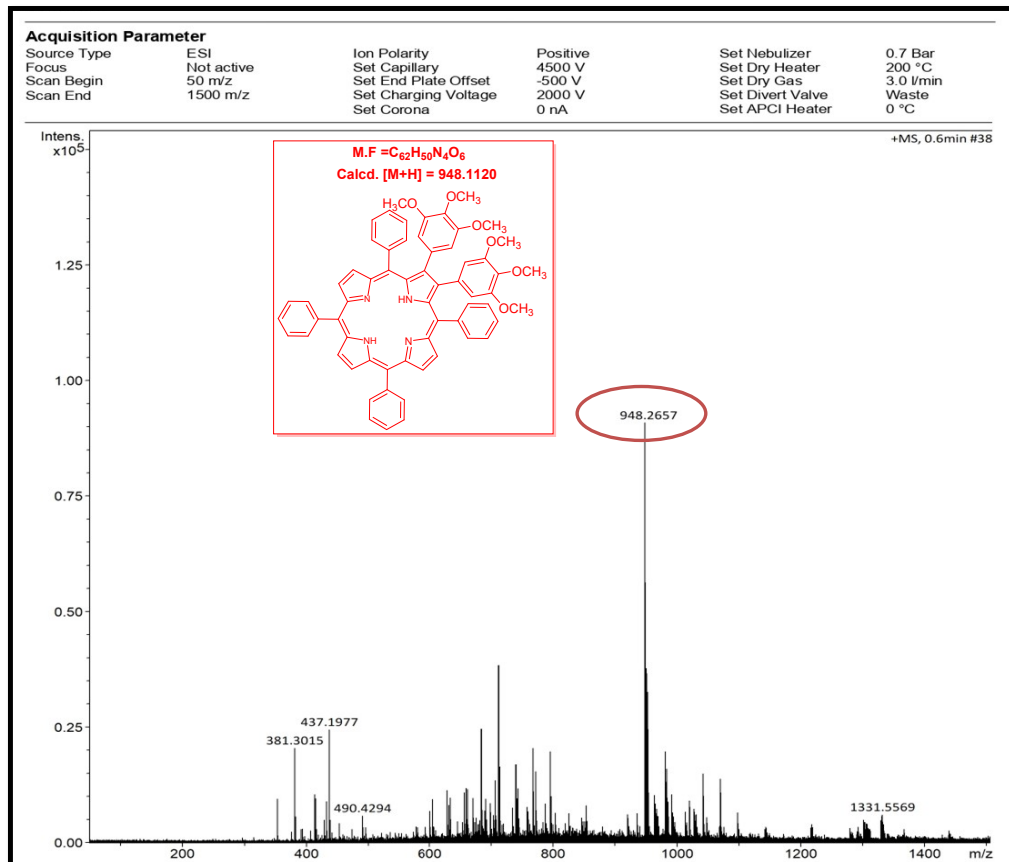


Figure S47. HRMS spectrum of ZnTPP(*m,p*-CH₃O-Ph)₂.

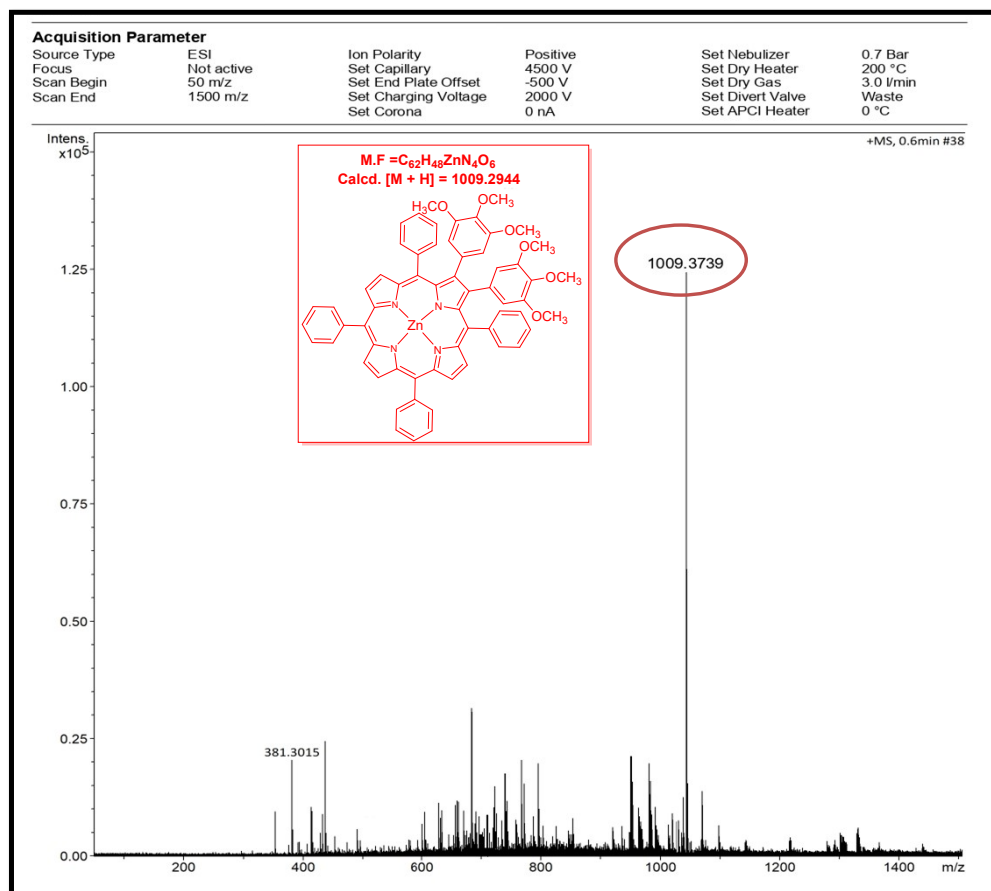


Figure S48. HRMS spectrum of NiTPP(*m,p*-CH₃O-Ph)₂.

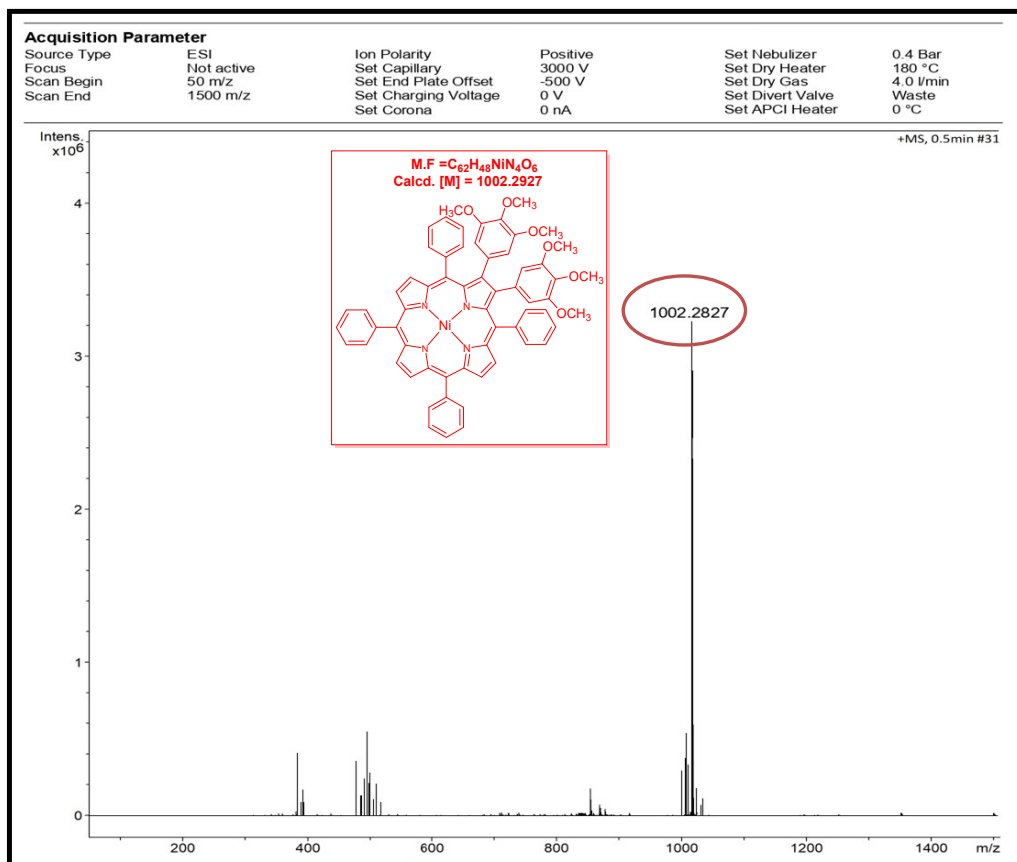


Figure S49. HRMS spectrum of CoTPP(*m,p*-CH₃O-Ph)₂.

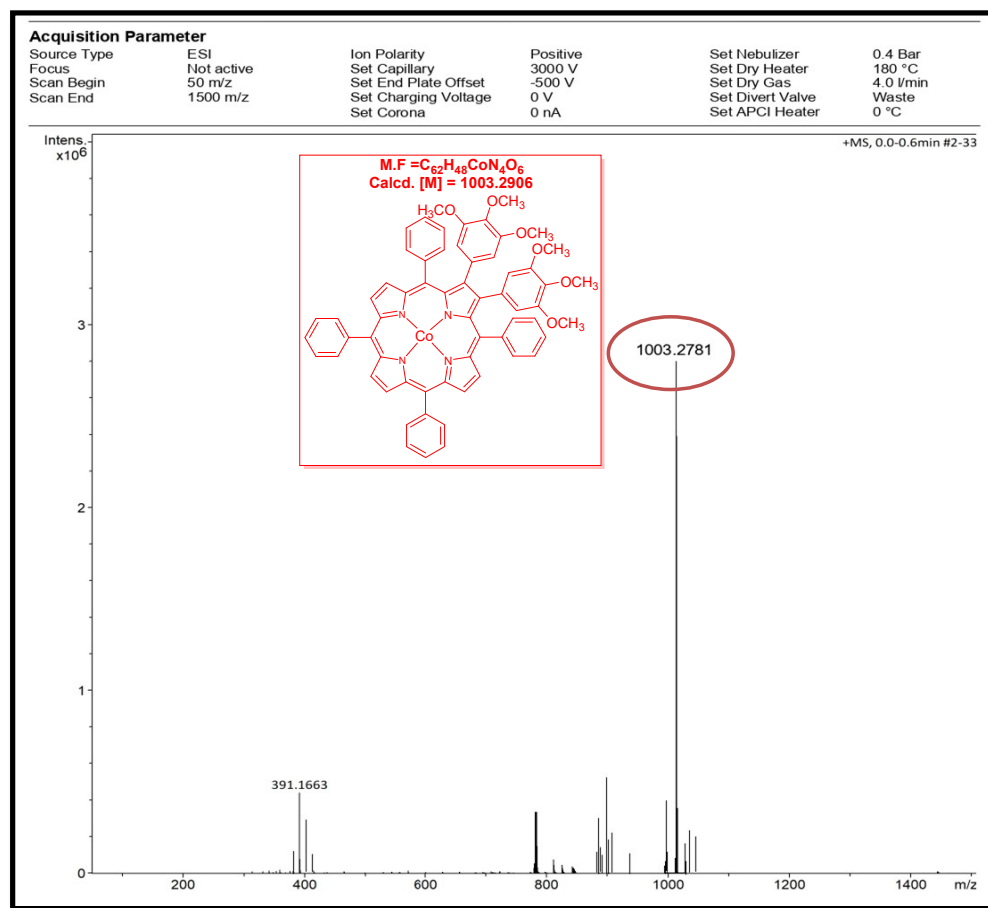


Figure S50. HRMS spectrum of CuTPP(*m,p*-CH₃O-Ph)₂.

